



Universiteit
Leiden
The Netherlands

The radiative efficiency of a radiatively inefficient accretion flow

D'Angelo, C.R.; Fridriksson, J.K.; Messenger, C.; Patruno, A.

Citation

D'Angelo, C. R., Fridriksson, J. K., Messenger, C., & Patruno, A. (2015). The radiative efficiency of a radiatively inefficient accretion flow. *Monthly Notices Of The Royal Astronomical Society*, 449(3), 2803-2817. doi:10.1093/mnras/stv465

Version: Not Applicable (or Unknown)

License: [Leiden University Non-exclusive license](#)

Downloaded from: <https://hdl.handle.net/1887/49412>

Note: To cite this publication please use the final published version (if applicable).

The radiative efficiency of a radiatively inefficient accretion flow

C. R. D’Angelo,^{1★} J. K. Fridriksson,² C. Messenger³ and A. Patruno^{1,4}

¹*Leiden Observatory, Leiden University, Postbus 9513, NL-2300 RA Leiden, the Netherlands*

²*Anton Pannekoek Institute for Astronomy, University of Amsterdam, Postbus 94249, NL-1080 GE Amsterdam, the Netherlands*

³*SUPA, School of Physics and Astronomy, University of Glasgow, Glasgow G12 8QQ, UK*

⁴*ASTRON, The Netherlands Institute for Radio Astronomy, Postbus 2, NL-7900 AA Dwingeloo, the Netherlands*

Accepted 2015 February 27. Received 2015 February 26; in original form 2014 October 14

ABSTRACT

A recent joint *XMM–Newton/Nuclear Spectroscopic Telescope Array (NuSTAR)* observation of the accreting neutron star Cen X-4 ($L_X \sim 10^{33}$ erg s⁻¹) revealed a hard power-law component ($\Gamma \sim 1–1.5$) with a relatively low cut-off energy (~ 10 keV), suggesting bremsstrahlung emission. The physical requirements for bremsstrahlung combined with other observed properties of Cen X-4 suggest the emission comes from a boundary layer rather than the accretion flow. The accretion flow itself is thus undetected (with an upper limit of $L_{\text{flow}} \lesssim 0.3L_X$). A deep search for coherent pulsations (which would indicate a strong magnetic field) places a 6 per cent upper limit on the fractional amplitude of pulsations, suggesting the flow is not magnetically regulated. Considering the expected energy balance between the accretion flow and the boundary layer for different values of the neutron star parameters (size, magnetic field, and spin) we use the upper limit on L_{flow} to set an upper limit of $\varepsilon \lesssim 0.3$ for the intrinsic radiative efficiency of the accretion flow for the most likely model of a fast-spinning, non-magnetic neutron star. The non-detection of the accretion flow provides the first direct evidence that this flow is indeed ‘radiatively inefficient’, i.e. most of the gravitational potential energy lost by the flow before it hits the star is not emitted as radiation.

Key words: accretion, accretion discs – stars: magnetic field – stars: neutron – X-rays: binaries – X-rays: individual: Cen X-4.

1 INTRODUCTION

It is still not established how accretion flows organize themselves at the very low luminosities observed in many accreting black hole and neutron star systems. When such sources are very bright [$L_X \gtrsim 10$ per cent of the Eddington luminosity; $L_{\text{Edd}} \equiv 4\pi GM_* m_p c / \sigma_T = 1.8 \times 10^{38} (M_*/1.4 M_\odot) \text{ erg s}^{-1}$] the accretion flow is an optically thick, geometrically thin accretion disc, as envisioned by early authors (Pringle & Rees 1972; Shakura & Sunyaev 1973), and the energy spectrum is dominated by a blackbody that peaks at hard ultraviolet energies (for supermassive black holes) or soft X-rays (for stellar mass black holes and neutron stars). This disc is *radiatively efficient*: the energy liberated by the inspiralling gas is efficiently radiated away. In a thin disc the luminosity scales linearly with the accretion rate. However, the luminosity of accreting black holes and neutron stars can vary by more than eight orders of magnitude. When the luminosity drops below 10^{-2} – $10^{-3} L_{\text{Edd}}$ the X-ray energy spectrum is dominated by a power law extending to high energies, typically $\gtrsim 50$ – 100 keV (e.g. Done, Gierliński & Kubota 2007). The optically thin gas that produces this component

is ~ 1000 times hotter than what the classic ‘thin disc’ (Shakura & Sunyaev 1973) solution would predict for the observed luminosity, but the geometry, large-scale dynamic behaviour, and accretion rate of the gas are uncertain.

More than 30 yr ago, Rees et al. (1982) proposed that this change in spectral behaviour in accreting black holes and neutron stars could be caused by a radical change in the accretion flow’s structure. They noted that below a critical density the accreting gas can no longer cool efficiently, so that the accretion flow will inflate vertically from a cool, dense thin disc into a much hotter, optically thin torus. As a result, the accretion flow becomes *radiatively inefficient*, which means that a large fraction of the gravitational potential energy in the gas is not lost to radiation but instead converted into some other form of energy (such as kinetic or internal potential energy). Since accreting black hole and neutron star accreting systems spend the vast majority of the time in this low-luminosity state, determining the physical structure and accretion rate of the flow is necessary to understand much of their evolution and influence on their environments, e.g. to predict black hole growth and spin evolution (from accreted matter) as well as feedback into their surroundings. In neutron stars, the relationship between luminosity and accretion rate is needed to understand the spin and mass evolution. Continued accretion at low rates can also produce emission from the

* E-mail: dangelo@strw.leidenuniv.nl

stellar surface, which complicates the interpretation of observations of quiescent neutron stars as evidence of deep crustal heating (e.g. Brown, Bildsten & Rutledge 1998).

Unfortunately there is no unique self-consistent dynamic model of a radiatively inefficient accretion flow (hereafter RIAF). The large scale height of the flow can result in large-scale radial and vertical gas motion, which can correspond to global energy and momentum transport, so that the local temperature and density of the flow become determined by the global flow properties. The uncertainty over energy transport relates closely to another major unsolved question: since the gas must lose a large amount of gravitational potential energy in order to accrete, where does the ‘hidden’ (i.e. non-radiated) energy go?

Since the early 1990s there has been considerable theoretical interest in RIAF solutions, mainly focused on black hole accretion. The most well known one is probably the ‘advection-dominated accretion flow’ (ADAF) solution (e.g. Narayan & Yi 1994), in which the majority of the accretion energy is advected inwards as protons in the gas are heated to virial temperatures. Other RIAF solutions propose a reduced mass accretion rate close to the central object. One popular set of solutions assumes that most of the energy liberated close to the central object is advected outward and is used to launch a strong outflow from the outer parts of the accretion flow (called ‘ADIOS’, or adiabatic inflow–outflow solution; Blandford & Begelman 1999; Begelman 2012). It has also been suggested that the flow could become ‘convection’ dominated (CDAF; with large-scale vertical or radial convection cells and a small net inward accretion rate; e.g. Quataert & Gruzinov 2000), or ‘magnetically’ dominated (in which a poloidal magnetic field is advected inwards from large distances and creates a magnetic barrier against accretion; Bisnovatyi-Kogan & Ruzmaikin 1974; Narayan, Igumenshchev & Abramowicz 2003). A considerable amount of accretion energy must also be used to launch the strong jets and outflows observed in the low-luminosity state of both black holes and neutron stars (e.g. Fender, Belloni & Gallo 2004; Markoff, Nowak & Wilms 2005).

The best observational constraint on the existence of a RIAF comes from Sgr A*, the black hole at the centre of the Galaxy. Sgr A* has a typical non-flaring luminosity of $L_X \sim 10^{33}$ erg s⁻¹, or about $10^{-11} L_{\text{Edd}}$ (for a mass of $4.1 \times 10^6 M_\odot$; Ghez et al. 2008). This is far below $L_X \sim 10^{41}$ erg s⁻¹, the luminosity corresponding to the inferred accretion rate of $10^{-5} M_\odot \text{ yr}^{-1}$ at the Bondi radius (estimated from the rate of gas capture from massive stellar winds in the Galactic Centre; e.g. Quataert & Gruzinov 2000). Both radio observations of the inner $100 R_S$ (Marrone et al. 2007) and X-ray observations of the inner $10^5 R_S$ around the black hole (Wang et al. 2013) show low-density gas consistent with being produced by a RIAF. ($R_S \equiv 2GM/c^2$ is the Schwarzschild radius corresponding to the event horizon of a non-spinning black hole of mass M). However, the central argument for a RIAF remains the strong imbalance between the accretion rate at the Bondi radius and the central luminosity. Without probing intermediate radii (where gas could be stored, as in transient binaries, or expelled) it is not possible to directly test the radiative inefficiency of the gas closest to the black hole.

Neutron stars in accreting binary systems show similar spectral and variability properties to those of black hole binaries (suggesting similar accretion physics), but unlike black holes have a hard surface where matter ultimately settles. The impact of gas with the surface will release a tremendous amount of energy which will likely be radiated efficiently away, so that the luminosity from the stellar surface should be a good proxy for the accretion rate on to the

star and hence in the innermost regions of the accretion flow (e.g. Narayan & Yi 1995). For example, if the majority of the accretion energy is advected inwards (ADAF) the surface of the neutron star will be much brighter than if the energy is used to expel gas in an outflow (as in e.g. ADIOS; Blandford & Begelman 1999). Indeed, the relative brightness of neutron star transients compared with black holes has been used as evidence of the existence of both an event horizon (Narayan, Garcia & McClintock 1997) and an ADAF (Done & Gierliński 2003).

Using neutron star binaries to constrain radiative efficiency requires understanding how the energy spectrum is produced. At very low luminosities in quiescent neutron star binaries, two spectral X-ray components are typically observed: a thermal (blackbody-like) one and a power-law one. It is generally accepted that the thermal component is produced by the neutron star surface, either as a result of heating by accreting gas or by nuclear processes in the deep crust (Brown et al. 1998). The power-law component most likely originates either in the boundary layer close to the neutron star or in the accretion flow itself (Menou et al. 1999).¹

If the power-law emission originated from a radiatively inefficient accretion flow, the neutron star surface (blackbody component) would be expected to be much brighter (potentially orders of magnitude) than the emission from the flow. In contrast, the thermal and power-law components for the faintest neutron star binaries (typically radiating at $\sim 10^{-5}$ – $10^{-6} L_{\text{Edd}}$) are often comparable (Campana et al. 1998; see also fig. 5 of Jonker et al. 2004). Furthermore, since the surface emission should be radiatively efficient, Menou et al. (1999) demonstrated that the very low luminosity from quiescent neutron stars requires a much lower mass transfer rate from the companion star than is expected from mass transfer models. To resolve this imbalance, they proposed that the fast-rotating magnetic field of these neutron stars expels most of the accretion flow (the ‘propeller’ scenario; Illarionov & Sunyaev 1975). The net accretion rate on to the star is thus several orders of magnitude lower than the accretion rate in the flow. Although they applied this idea to the ADAF model in particular, a strong propeller (or some other mechanism to expel gas that is unrelated to the accretion flow) is generically required for any radiatively inefficient flow if the power-law component is generated by the accretion flow, otherwise the surface will be much brighter than the flow. However, many low-luminosity neutron star binaries show no signs of magnetic activity (such as X-ray pulsations), and recent work has demonstrated that the magnetic field required for the ‘propeller’ scenario to work in quiescent neutron stars is about 10 times as large as those in accreting millisecond X-ray pulsars, where pulsations are seen (Bernardini et al. 2013).

A recent observation of a nearby accreting neutron star, Cen X-4, has offered new insights into the accretion properties of low-luminosity neutron star binaries. In simultaneous *Nuclear Spectroscopic Telescope Array* (*NuSTAR*) and *XMM-Newton* observations of Cen X-4 in 2013 January, Chakrabarty et al. (2014) found evidence of a break or cut-off in the hard X-rays around 10 keV, while the index of the power-law component below 10 keV was quite hard: $\Gamma \sim 1$ – 1.5 . They considered different physical scenarios for the origin of the high-energy emission, before focusing on a scenario in which the spectrum is produced by bremsstrahlung

¹ An alternative suggestion – that the quiescent X-ray emission comes from the impact of a pulsar wind from the neutron star with the outer accretion disc (Campana & Stella 2000) – has been disfavoured by more recent observations (Bernardini et al. 2013; Chakrabarty et al. 2014).

radiation from a hot massive outflow at a large distance from the star, roughly as predicted by the model suggested by Blandford & Begelman (1999).

In this paper, we propose that the power-law component seen in Cen X-4 and similar quiescent neutron star binaries is most plausibly produced by bremsstrahlung emission from the boundary layer on the surface of the star. This suggests that *all* the observed emission is coming from near the surface of the star, and the power-law and thermal components are directly coupled. Our interpretation naturally fits the observed spectrum, and also explains the energy balance and covariation of the two components without invoking a magnetic propeller. Most significantly, if all the observed emission comes from a boundary layer, then the flow itself is completely undetected, i.e. it is indeed radiatively inefficient. This would be the most direct, model-independent evidence for radiative inefficiency in any accreting system.

The paper is organized as follows. In Section 2 we review how much emission is expected to come from a neutron star boundary layer and accretion flow, and how the neutron star's properties affect this balance. In Section 3 we summarize the observed properties of Cen X-4 and present a partial reanalysis of the data presented in Chakrabarty et al. (2014) in order to constrain the presence of an additional spectral component. We also present the results of a search for coherent pulsations (which would indicate magnetically channelled accretion). In Section 4 we reinvestigate the accretion-flow model proposed by Chakrabarty et al. (2014) and outline its difficulties in explaining the observation. We then demonstrate that the most plausible model for the power-law component is bremsstrahlung from the star's surface. We also set limits on the scale height and density of the boundary layer. (A more complete analysis of the physical constraints on the boundary layer imposed by this observation will follow in a separate paper.) Finally, in Section 4.3 we calculate upper limits for the intrinsic radiative efficiency of the accretion flow, building on the spectral analysis presented in Section 3. In Sections 5 and 6 we discuss briefly the implications of our results, summarize our conclusions, and explore how future observations of low-level accretion on to neutron stars can be used to put better constraints on the radiative efficiency of the accretion flow.

2 HOW ACCRETION ENERGY IS LIBERATED IN NEUTRON STARS

What fraction of the infalling gas's gravitational potential energy will be converted to radiation in the boundary layer of the neutron star? This question is central to the argument of this paper: to put constraints on the intrinsic radiative efficiency of the accretion flow (i.e. the amount of gravitational potential energy that the accretion flow itself radiates away), we need to know how much energy is still stored in the gas when it reaches the boundary layer. The division of energy between the boundary layer and accretion flow can be altered both by the properties of the neutron star (its size, spin, and magnetic field, as described in Sections 2.2 and 2.3) and by the properties of the boundary layer and accretion flow.

The total rate of gravitational potential energy released in a Newtonian potential by matter accreting at a rate \dot{M} on to a star of mass M_* and radius R_* is

$$\dot{E}_{\text{pot}} = \frac{GM_*\dot{M}}{R_*}, \quad (1)$$

which can be divided into the fraction of energy available to be radiated by the flow, $\mathcal{F}_{\text{flow}}$, and the boundary layer, \mathcal{F}_{bl} .²

In this paper we define the boundary layer as the radius where the angular frequency of the gas reaches a maximum, usually very close to the star, so that $b/R_* \ll 1$, where b is the width of the layer (Shakura & Sunyaev 1973; Frank, King & Raine 2002). Provided that the accretion flow remains nearly Keplerian, the kinetic energy of a test particle at the boundary layer is $\sim 0.5mv_{\text{K},*}^2$ (where $v_{\text{K},*}$ is the Keplerian velocity at the star's surface), which will mainly be converted to radiation when it hits the star. As long as the boundary layer is very thin, the two components \mathcal{F}_{bl} and $\mathcal{F}_{\text{flow}}$ will thus be roughly equal, so that $\mathcal{F}_{\text{bl}} \simeq \mathcal{F}_{\text{flow}} \simeq 0.5$ (e.g. Frank et al. 2002). However, if the boundary layer is *not* thin, and $b \gtrsim R_*$, the gas will also have additional gravitational potential energy $GM_*m/(R_* + b)$ at the top of the boundary layer, which will then change the balance between $\mathcal{F}_{\text{flow}}$ and \mathcal{F}_{bl} , increasing \mathcal{F}_{bl} by a factor $(R_* + b)/R_*$ (Popham & Sunyaev 2001). If the boundary layer is very physically extended the flow will thus contribute much less radiation to the total spectrum, making it harder to establish that the accretion flow is intrinsically radiatively inefficient.

2.1 How thick is the boundary layer?

At low accretion rates the assumption that $b \ll R_*$ may not be valid. In their study of accretion on to white dwarfs, Narayan & Popham (1993) found that the boundary layer thickness can increase substantially as \dot{M} decreases, mainly due to a thermal instability that causes the boundary layer to heat up and expand. However, their results (and the later study of neutron star boundary layers of Popham & Sunyaev 2001) may have considerably overestimated the boundary layer temperature due to an incomplete treatment of radiative cooling (Grebenev & Sunyaev 2002), thus overestimating the boundary layer thickness. Observations of neutron star low-mass X-ray binaries (LMXBs) suggest that the boundary layer becomes optically thin below $\sim 0.01 L_{\text{Edd}}$, as evinced by the lack of a strong blackbody component in the X-ray spectrum (e.g. Revnivtsev et al. 1999), which would also suggest an extended, optically thin boundary layer. To our knowledge, no theoretical work has studied the formation of a boundary layer at the low accretion rates seen in Cen X-4, so it is difficult to make anything more than basic predictions for boundary layer thickness.

In this paper our aim is to demonstrate that the accretion flow in Cen X-4 is radiatively inefficient. We therefore consider limits on what the boundary layer properties would be assuming the flow is radiatively efficient, which can then be excluded by observation. Following the logic for standard (thin) accretion discs, in the boundary layer the gas must rapidly decelerate from nearly Keplerian orbits to corotation with the star. As long as the net infall velocity is not strongly supersonic, the gas pressure gradient must balance the gravitational force, so that

$$b \simeq \frac{c_s^2}{v_{\text{K},*}^2} R_* \quad (2)$$

(where c_s is the gas's sound speed; Frank et al. 2002). If the protons and electrons in the gas are efficiently coupled, then the temperature

² Note that throughout this paper we define radiative efficiency \mathcal{F} as the fraction of gravitational potential energy released as radiation. This is a different quantity from L/Mc^2 , the fraction of the accretion flow's *rest-mass energy* that is radiated, which is also sometimes called the 'radiative efficiency' of an accretion flow (and is ~ 10 per cent for a black hole).

of the entire gas is constrained by the *NuSTAR* observation to be ~ 18 keV (Chakrabarty et al. 2014), corresponding to $b \sim 10^2$ cm. However, if the electrons and protons are not efficiently coupled, the proton temperature could be much larger – of order the virial temperature. In this case,

$$c_s^2 \sim \frac{\alpha v_{K,*}^2}{5} \quad (3)$$

(e.g. King & Lasota 1987), so that $b \sim 0.2\alpha R_*$, where $\alpha < 1$ is the standard viscosity parameter. We thus assume that, provided that the flow is quasi-Keplerian close to the star, the boundary layer will remain small compared with the radius of the star, so that $\mathcal{F}_{\text{bl}} \simeq \mathcal{F}_{\text{flow}} \simeq 0.5$.

2.2 Accretion on to a magnetosphere at low \dot{M}

The largest potential influence on the boundary layer/accretion flow energy balance will come from a strong stellar magnetic field. A sketch of a RIAF accreting on to a star with a strong magnetic field is shown in Fig. 1. Accretion from a RIAF on to a magnetosphere has not been theoretically investigated, but the basic physics should be similar to magnetospheric accretion from a disc. The magnetic field will truncate the inner part of the accretion flow at the ‘magnetospheric radius’ r_m and channel accreting material on to the pole of the star (e.g. Pringle & Rees 1972; Ghosh, Pethick & Lamb 1977). The inner magnetosphere will be nearly evacuated of gas, while the stellar surface will be significantly brighter than for a non-magnetic star. The interaction between the disc and the field will also allow an exchange of angular momentum between the star and the flow.

The magnetic field has two effects on the energy balance between the flow and the boundary layer. First, since the inner edge of the flow (r_m) is now much further from the star, $\mathcal{F}_{\text{flow}}$ will be reduced by R_*/r_m . Second, if the star is spinning much faster than the inner edge of the disc, the relative spin rate of the magnetic field and inner accretion flow can launch an outflow of gas from the disc (the ‘propeller’ effect; Illarionov & Sunyaev 1975). This will dramatically reduce accretion on to the neutron star’s surface, and thus \mathcal{F}_{bl} and the luminosity of the boundary layer.

In an accretion flow surrounding a strong stellar magnetic field, the inner edge can be defined as the point where the magnetic field is

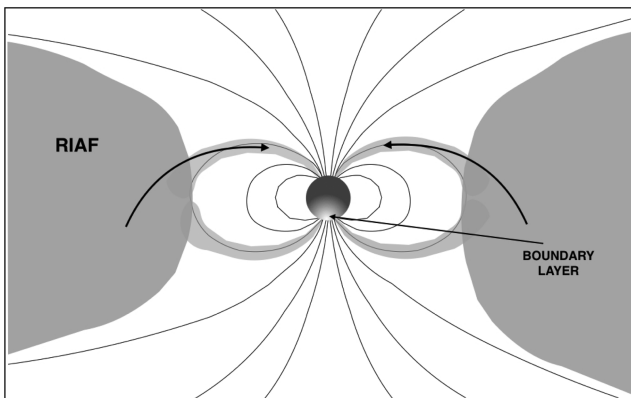


Figure 1. Schematic illustration of accretion from a radiatively inefficient flow on to a strong magnetic field. MHD simulations suggest that the magnetic field will adopt a mainly open configuration, with limited connection between the star and the flow. Since the flow does not radiate efficiently while the boundary layer does, emission from the flow is not detected, while accretion on to the boundary layer produces the observed X-ray spectrum in quiescent neutron stars.

strong enough to enforce corotation of gas (Spruit & Taam 1993):

$$\begin{aligned} r_m &= \left(\frac{\eta \mu^2}{4\Omega_* \dot{M}} \right)^{1/5} \\ &= 2.4 \times 10^6 \eta^{1/5} \left(\frac{B_*}{10^8 \text{ G}} \right)^{2/5} \left(\frac{R_*}{10^6 \text{ cm}} \right)^{6/5} \\ &\quad \times \left(\frac{P_*}{2 \times 10^{-3} \text{ s}} \right)^{1/5} \left(\frac{\dot{M}}{10^{16} \text{ g s}^{-1}} \right)^{-1/5} \text{ cm}. \end{aligned} \quad (4)$$

In this equation, $\mu = B_* R_*^3$ is the magnetic moment of the star, and $\eta \leq 1$ is a dimensionless parameter characterizing the strength of the toroidal magnetic field induced by the relative rotation between the disc and dipolar magnetic field. $\Omega_*(P_*)$ is the star’s angular spin frequency (period) and \dot{M} the mass accretion rate through the disc. The magnetospheric radius is scaled for a rapidly spinning, weakly magnetized neutron star in outburst (at $\sim 0.01 \dot{M}_{\text{Edd}}$, or $L_X \sim 1.8 \times 10^{36}$ erg s^{-1}). Throughout this paper, we assume a neutron star of $1.4 M_\odot$ and a radius of 10^6 cm.³

2.2.1 The magnetic ‘propeller’ model

The biggest uncertainty in establishing \mathcal{F}_{bl} and $\mathcal{F}_{\text{flow}}$ is determining what happens if the magnetic field of the star spins faster than the inner edge of the accretion flow. This can happen when the accretion rate decreases enough that r_m (given by equation 4) lies outside the corotation radius, $r_c \equiv (GM_*/\Omega_*^2)^{1/3}$, where the Keplerian disc and star rotate at the same rate. In this case, the rotating magnetic field acts as a centrifugal barrier, preventing matter from accreting on to the star. It is often assumed that the majority of matter accreting through the disc will be expelled when it hits this centrifugal barrier (the ‘propeller’ mechanism; Illarionov & Sunyaev 1975), thus dramatically reducing \mathcal{F}_{bl} .

A considerable uncertainty in the propeller model is how much gas (if any) is actually accreted on to the star. Some authors have assumed that once $r_m > r_c$ all the gas is expelled in an outflow, so that only the accretion flow itself is visible (e.g. Stella et al. 1994). In contrast, magnetohydrodynamics (MHD) simulations of the strong propeller regime tend to show variable accretion episodes, where a considerable amount of mass is periodically accreted on to the star (Romanova et al. 2004; Ustyugova et al. 2006; Lii et al. 2014). In simulations the amount of gas accreted on to the surface decreases as the propeller gets ‘stronger’ (i.e. the accretion rate decreases and r_m moves further from r_c). In their interpretation of the Cen X-4 quiescent spectrum Menou & McClintock (2001) also assumed some gas accretes on to the star. Since Cen X-4’s large, variable blackbody component (interpreted as emission from the stellar surface) is most likely produced by accretion, the propeller solution can only apply if some gas accretes on to the star. In our investigation of how the radiative balance between the star and the flow is affected by a strong propeller, we use the results of simulations by Ustyugova et al. (2006) and Lii et al. (2014).

³ Equation (4) predicts a somewhat smaller truncation radius than the more commonly used prescription (Pringle & Rees 1972; Ghosh et al. 1977) which equates the ram pressure of the infalling gas and magnetic pressure of the magnetic field of the star without considering the relative rotation between the two components. An uncertainty of at least ~ 2 – 3 for r_m should be assumed.

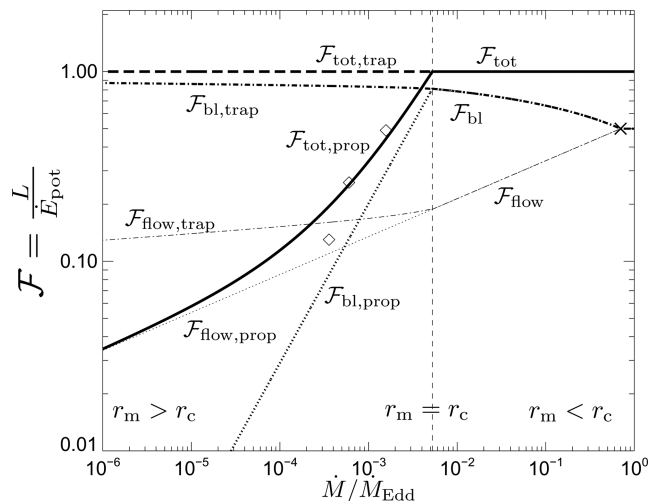


Figure 2. Radiative efficiency (\mathcal{F}) of a 2-ms pulsar with a field of 10^8 G for both the propeller and trapped disc models. The radiative efficiency of the boundary layer (bl) and flow (flow) is shown as a function of accretion rate. At high accretion rates ($r_m < r_c$), the two models are equivalent. Above $\dot{M} \simeq 0.7 \dot{M}_{\text{Edd}}$ the two radiative components are equal since the flow reaches the star (disregarding the effects from Sections 2.3.1 and 2.3.2). Below $\simeq 0.7 \dot{M}_{\text{Edd}}$ the magnetosphere is strong enough to truncate the disc, increasing \mathcal{F}_{bl} and decreasing $\mathcal{F}_{\text{flow}}$. At low accretion rates ($\dot{M} \lesssim 5 \times 10^{-3} \dot{M}_{\text{Edd}}$), the radiative efficiency is very different for the trapped disc [thin (flow) and thick (boundary layer) dot-dashed curves; thick dashed curve (total); D’Angelo & Spruit 2012 and when a propeller forms [thin (flow) and thick (boundary layer) dotted curve; thick solid curve (total)]. The propeller model used to estimate $\mathcal{F}_{\text{bl,prop}}$ and $\mathcal{F}_{\text{flow,prop}}$ is from Ustyugova et al. (2006), and the diamond points show $\mathcal{F}_{\text{bl,prop}}$ from Lii et al. (2014). In a trapped disc, the inner edge of the disc stays close to the corotation radius as \dot{M} in the disc decreases, so that gas can always be accreted on to the star. In contrast, when $r_m > r_c$ in the propeller scenario, most gas in the disc is expelled rather than accreted, so the radiative efficiency decreases strongly as a function of \dot{M} .

2.2.2 The trapped disc

Recent work investigating the interaction between a magnetosphere and an accretion disc has suggested that a strong propellered outflow may not easily form when $r_m > r_c$ (Spruit & Taam 1993; D’Angelo & Spruit 2010). This is because in order to efficiently drive an outflow r_m must lie significantly outside r_c , otherwise the differential rotation between the disc and star is not large enough to accelerate the majority of the infalling gas to its escape velocity (Spruit & Taam 1993). Instead, the disc–field interaction can keep matter confined in the disc, and the angular momentum added by the disc–field interaction at the inner edge of the disc is carried outward via turbulent viscosity. As a result, some matter can continue to accrete on to the star even when the accretion rate is very low, and a strong propeller outflow does not form. D’Angelo & Spruit (2010) named such discs ‘trapped discs’, since the inner edge of the disc remains trapped near r_c by the interaction between the disc and the magnetosphere. This can lead to episodic bursts of accretion (Spruit & Taam 1993; D’Angelo & Spruit 2010, 2012) as well as efficient spin-down of the star (D’Angelo & Spruit 2011).

The angular momentum from the star added at r_m alters the radial density distribution in the disc. If there is no accretion at all through the disc the density distribution approaches a ‘dead disc’, so-called by Sunyaev & Shakura (1977), who first derived it. In a ‘dead disc’ density distribution, the torque added by the magnetic field at r_m matches the rate at which angular momentum is carried outward by

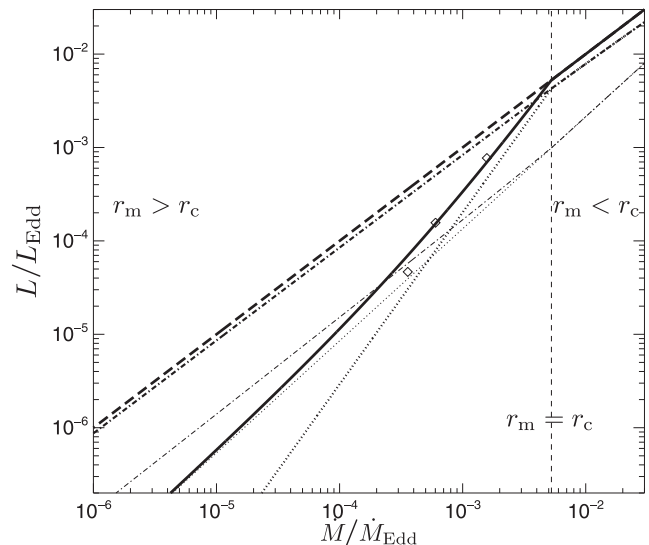


Figure 3. Luminosity as a function of accretion rate (assuming a radiatively efficient accretion flow) for different spectral components in a trapped disc and propeller scenario. The curve coding is the same as in Fig. 2. As the accretion rate decreases, the luminosity of a trapped disc is dominated by the surface component (since the accretion flow is truncated), while in a propeller it is dominated by the accretion flow (since very little gas is accreted on to the star).

viscous processes through the disc, so that the net accretion rate on to the star is zero.

The trapped disc density solution is the sum of an accreting component and a ‘dead disc’ component. As the net accretion rate through the disc decreases r_m remains ‘trapped’ very close to r_c and the density profile approaches a dead disc one. The ‘trapped disc’ is therefore the opposite extreme of the propeller: the angular momentum from the star is added to the disc rather than expelled in an outflow, and most of the gas in the disc is ultimately accreted on to the star. Trapped discs have not yet been properly explored with numerical simulations, although some evidence of disc trapping was observed in the ‘weak propeller’ MHD simulations reported by Ustyugova et al. (2006).

The propeller and trapped disc scenarios result in very different predictions for how \mathcal{F}_{bl} and $\mathcal{F}_{\text{flow}}$ change with accretion rate. If there is a strong propeller, only a small amount of gas reaches the stellar surface, so that \mathcal{F}_{bl} is much smaller than $\mathcal{F}_{\text{flow}}$. In a trapped disc the opposite is true: $\mathcal{F}_{\text{flow}}$ is much smaller than \mathcal{F}_{bl} because the flow is truncated by the field at a considerable distance from the star.

Fig. 2 shows the evolution of \mathcal{F}_{bl} , $\mathcal{F}_{\text{flow}}$, and $\mathcal{F}_{\text{tot}} = \mathcal{F}_{\text{bl}} + \mathcal{F}_{\text{flow}}$ as a function of accretion rate for a propeller and trapped disc. In this figure we use a weakly magnetized ($B = 10^8$ G) neutron star with a high spin rate ($P = 2$ ms) as our reference model, so that $r_m \sim r_c \sim 30$ km for $\dot{M}/\dot{M}_{\text{Edd}} \sim 4 \times 10^{-3}$. We use the trapped disc model presented by D’Angelo & Spruit (2011) (with $\Delta R/R = \Delta R_2/R = 0.1$ and $\eta = 1$; see paper for details of the numerical parameters). For the propeller regime we use the MHD simulations reported by Ustyugova et al. (2006), who empirically fit the results of simulations of propeller discs of different mean accretion rate to derive a relationship between the mean \dot{M} through the disc and the net \dot{M} on to the star (and hence \mathcal{F}_{bl}). The diamond symbols show \mathcal{F}_{bl} as found by more recent simulations by Lii et al. (2014). The discrepancy between the simulations stresses the large

uncertainty in how much mass is actually accreted on to the star in the propeller scenario.

Beginning with the highest accretion rates ($>0.7 \dot{M}_{\text{Edd}}$), the accretion flow overwhelms the magnetic field and gas accretes directly on to the star. When $\dot{M} \sim 0.7 \dot{M}_{\text{Edd}}$ (the ‘ \times ’ in Fig. 2), the magnetic field is strong enough to disrupt the flow so that \mathcal{F}_{bl} increases and $\mathcal{F}_{\text{flow}}$ decreases as \dot{M} decreases, following from equation (4). As the accretion rate drops further and $r_{\text{m}} = r_{\text{c}}$, the two possible solutions (trapped disc or propeller) begin to diverge.

In the ‘propeller’ scenario (shown in Fig. 2 as thick [\mathcal{F}_{bl}] and thin [$\mathcal{F}_{\text{flow}}$] dotted curves), $\mathcal{F}_{\text{flow}} \propto \dot{M}^{1/5}$, since the inner disc edge moves outward as \dot{M} decreases. The surface component, \mathcal{F}_{bl} , will decline steeply with decreasing \dot{M} , since the propeller becomes stronger with decreasing \dot{M} and less gas hits the stellar surface. $\mathcal{F}_{\text{flow}}$ will decrease by a factor of 14 if the accretion rate decreases from the Eddington rate by a factor of 10^6 , and \mathcal{F}_{bl} by more than 800 times so the radiative contribution from the stellar surface will be completely negligible if the accretion flow is intrinsically radiatively efficient. The total available energy for radiating $\mathcal{F}_{\text{flow}} + \mathcal{F}_{\text{bl}}$ (the thick solid line) thus decreases rapidly with decreasing \dot{M} . Note that in a propeller, if \dot{M} decreases from \dot{M}_{Edd} to $10^{-6} \dot{M}_{\text{Edd}}$, r_{m} will increase from $\sim r_{*}$ to $\sim 5 r_{\text{c}}$, meaning that the star would be spinning 10 times as fast as the inner edge of the disc.

In contrast to the propeller, in the trapped disc at low \dot{M} , \mathcal{F}_{bl} and $\mathcal{F}_{\text{flow}}$ remain approximately constant as \dot{M} decreases (shown, respectively, by the thick and thin dot–dashed curves in Fig. 2), and $\mathcal{F}_{\text{bl}} + \mathcal{F}_{\text{flow}} = 1$ (thick dashed curve) for all accretion rates (since all gas ends up on the stellar surface). The ratio between \mathcal{F}_{bl} and $\mathcal{F}_{\text{flow}}$ stays roughly constant because the disc–field interaction ‘traps’ the disc near r_{c} , while gas continues to penetrate through the centrifugal barrier and accrete on to the star.

Fig. 3 shows the luminosity of the flow and the boundary layer in both a propelling disc and trapped disc as function of \dot{M} . This assumes both the surface and the flow radiate efficiently, so the only difference comes from the amount of energy in each component, \mathcal{F}_{bl} and $\mathcal{F}_{\text{flow}}$. The curves are the same as in Fig. 2. In a trapped disc, the luminosity is dominated by the surface emission, since the inner disc is truncated by the magnetosphere. In contrast, most of the emission in a propelling disc comes from the accretion flow, since the majority of the gas is expelled from the disc before it can accrete on to the star.

Do Cen X-4 and other quiescent neutron stars have a strong magnetic propeller? The strong, fluctuating quasi-blackbody X-ray component most likely arises from the matter hitting the surface of the star, so the strength of this component can be used to estimate how much matter reaches the surface. In Cen X-4, the power-law X-ray component is nearly as bright as the thermal component (and they are of similar orders of magnitude in several other quiescent sources; Campana et al. 1998). If the power-law component is produced by radiatively inefficient gas in the accretion flow, there must therefore be a strong propeller effect, since otherwise the blackbody component would be much brighter than the accretion flow. In this case, the near balance between thermal and power-law emission is a complete coincidence: the propeller expels just enough gas (in Cen X-4 and other sources) so that the radiatively efficient accretion on to the surface of the star is as bright as the radiatively inefficient accretion flow. This is true for any RIAF model. Since the relative contribution of each spectral component in Cen X-4 stays roughly constant with luminosity (while the luminosity change by a factor of 10), the ‘propeller’ efficiency would also have to scale with accretion rate in the same way as the RIAF luminosity as the accretion rate changes by an order of magnitude.

If instead a trapped disc forms, there is no outflow and \mathcal{F}_{bl} and $\mathcal{F}_{\text{flow}}$ are approximately independent of \dot{M} , so that the accretion rate on to the star matches that in the flow. In this case it is unlikely that the power-law component originates in the flow, since Fig. 2 shows that much less accretion energy is available for radiation than in the stellar surface, whereas Cen X-4 shows roughly equal contributions from both components.

The power-law component could originate in the boundary layer. In this case, a strong propeller effect would require a more radiatively inefficient accretion flow, since the accretion rate in the flow would be much higher than the amount of gas that actually ends up on the star. By assuming there is no propeller, the non-detection of the accretion flow thus sets a robust *upper limit* on the intrinsic radiative efficiency of the flow.

2.3 Other effects on radiative efficiency

2.3.1 Neutron star size

In the absence of a neutron star magnetic field, the accretion flow will extend close to the neutron star’s surface and general relativity is needed to determine the energy balance between the accretion flow and boundary layer. This has been discussed in some detail first by Sunyaev & Shakura (1986) and Shakura & Sunyaev (1988) (who dealt chiefly with non-spinning neutron stars), and more recently in Sibgatullin & Sunyaev (1998), who consider a rapidly spinning neutron star.

The neutron star radius can be smaller than the innermost stable circular orbit – the smallest radius for which bound orbits exist in a (non-spinning) Schwarzschild metric, $R_{*} < R_{\text{isco}} = 3 R_{\text{S}}$. Inside this orbit the gas will be decoupled from the rest of the accretion flow and will fall chaotically on to the surface of the star. As a result, the boundary layer will be brighter and the accretion flow dimmer than if the disc extended to the stellar surface. Sunyaev & Shakura (1986) calculated the energy released in the flow and the boundary layer in a Schwarzschild metric. Expressed as first-order corrections to the energy balance in Newtonian gravity, the fraction of energy from the boundary layer and flow will be

$$\begin{aligned} \mathcal{F}_{\text{bl}} &\simeq 0.5 \left(1 + \frac{R_{\text{S}}}{R_{*}} \right), \\ \mathcal{F}_{\text{flow}} &\simeq 0.5 \left(1 - \frac{R_{\text{S}}}{2 R_{*}} \right). \end{aligned} \quad (5)$$

The uncertainty in the neutron star internal equation of state introduces uncertainty in $\mathcal{F}_{\text{bl}}/\mathcal{F}_{\text{flow}}$, but even over the entire range of viable equations of state, this effect will be small except for very soft equations of state. From consulting e.g. fig. 2 of Lattimer & Prakash (2001), a $2 M_{\odot}$ star (where the effect is largest) will have $\mathcal{F}_{\text{bl}}/\mathcal{F}_{\text{flow}} = 1.8\text{--}2.1$, while for a $1.5 M_{\odot}$ star $\mathcal{F}_{\text{bl}}/\mathcal{F}_{\text{flow}} < 1.8$. If the star is spinning very rapidly, the Schwarzschild metric is no longer applicable and R_{isco} will be smaller, further reducing the imbalance between \mathcal{F}_{bl} and $\mathcal{F}_{\text{flow}}$. Even for a massive non-spinning neutron star and very soft equation of state this effect is thus small.

2.3.2 Spinning near break-up

If the inner edge of the accretion flow reaches the stellar surface and the star spins near break-up, angular momentum exchange between star and disc will also influence the relative flux contributions from the flow and the stellar surface (Paczynski 1991; Popham & Narayan 1991). As the star approaches its break-up frequency (~ 1230 Hz

for a $1.4 M_{\odot}$, 10 km neutron star; Cardall, Prakash & Lattimer 2001), the inner boundary of the disc must transport stellar angular momentum outward from the star in order for accretion to continue (known as a ‘maximally torqued’ inner boundary condition). Popham & Narayan (1991) and Paczynski (1991) demonstrated that this increases the fraction of energy released in the flow to $\mathcal{F}_{\text{flow}} \simeq 0.75$.

As gas hits the surface of the star, some of its kinetic energy will be used to increase the star’s rotation rate (e.g. Frank et al. 2002). As the star’s spin increases this energy becomes considerable, and decreases the fraction of energy released as radiation by the boundary layer:

$$\mathcal{F}_{\text{bl}} = \frac{1}{2} \left(1 - \frac{\Omega_*}{\Omega_{\text{K},*}} \right)^2, \quad (6)$$

where $\Omega_{\text{K},*}$ is the Keplerian frequency at the stellar surface. Although in principle rapid rotation could considerably reduce radiation from the boundary layer, the fastest confirmed millisecond pulsar has a spin frequency of 716 Hz (Hessels et al. 2006), which will reduce the boundary layer luminosity by about a factor of 2 compared with a non-spinning star. The spin frequency of a neutron star might also be limited by gravitational wave emission (Bildsten 1998) or regulation by the magnetic field (Patruno, Haskell & D’Angelo 2012) above ~ 1000 Hz, the effect of spin rate will likely not influence the surface/disc luminosity balance by more than a factor of ~ 2 – 3 . In Cen X-4, the history of strong accretion outbursts (which would increase the stellar spin rate) and non-detection of a magnetic field (which if present could spin down the star), both suggest a fast spin period, which would lead to reduced energy release from the boundary layer. If only the boundary layer is detected in the X-ray spectrum (and there is no substantial magnetic field), a rapid spin implies that the accretion flow is even more radiatively inefficient than if Cen X-4 is a slow rotator.

Without any constraints on the size, spin, or magnetic field for the neutron star, there is thus considerable uncertainty in the possible energy balance between the accretion flow and the boundary layer, which will add uncertainty to any attempt to constrain the intrinsic radiative efficiency of the accretion flow. However, as we outline in Section 4.3, even within these uncertainties, a reasonably small measured upper limit on L_{flow} can still put some constraints on the intrinsic radiative efficiency of the flow.

3 OBSERVATIONS OF CEN X-4

Cen X-4 is the brightest quiescent neutron star LMXB, and was last observed in outburst in 1979 (Kaluzienski, Holt & Swank 1980). Based on observed X-ray bursts Chevalier et al. (1989) derived a distance upper limit of 1.2 ± 0.3 kpc (see also González Hernández et al. 2005; Kuulkers, in’t Zand & Lasota 2009). The orbital period of the binary is 15.1 h (Chevalier et al. 1989), and the companion is thought to be of spectral type K3–K7 V (Torres et al. 2002; D’Avanzo et al. 2005). The source has a typical X-ray luminosity of $\sim 10^{32}$ erg s $^{-1}$, but is variable on a wide range of time-scales. It shows correlated X-ray, UV, and optical variability on time-scales down to at least ~ 100 s, and a change of more than factor of 20 in 0.5–10 keV luminosity has been observed over a few days (Bernardini et al. 2013). As mentioned above, the 0.5–10 keV spectrum shows two components – a soft blackbody-like component and a harder component well fitted by a power law with photon index $\Gamma \sim 1$ – 2 – which vary together and contribute roughly equal amounts of flux (Cackett et al. 2010, 2013; Bernardini et al. 2013). The relative proximity of the source means that a high-quality X-

ray spectrum can be obtained even in quiescence, providing a rare opportunity to study accretion at very low luminosities in detail.

We have reanalysed the simultaneous *XMM-Newton* and *NuSTAR* observations of Cen X-4 performed in 2013 and reported in Chakrabarty et al. (2014), in order to put upper limits on the strength of the undetected accretion flow. In Section 3.1 we describe the basic data extraction and spectral fitting we performed; in Section 4.3 we then use these results to test for the possible presence of an additional spectral component from the accretion flow. The analysis procedure and results we present in Section 3.1 are largely equivalent to those in Chakrabarty et al. (2014), who provide a much more detailed description and in-depth analysis of the data.

We have also used a 2003 archival *XMM-Newton* observation of Cen X-4 to perform a deep search for coherent pulsations that would indicate a relatively strong magnetic field (and suggest a magnetic propeller). We describe this search in Section 3.2.

3.1 Spectral analysis

We analysed the *XMM-Newton* European Photon Imaging Camera (EPIC; Jansen et al. 2001; Strüder et al. 2001; Turner et al. 2001) data of Cen X-4 (ObsID 0692790201) with the *SAS* software, version 13.5.0, and the latest available calibration files (in 2014 August). We reprocessed the raw MOS and pn data with the *EMPROC* and *EPPROC* tasks, in the latter case incorporating a correction for the effects of X-ray loading on the pn data with *EPXRLCORR*. We also applied a correction for spatially dependent charge-transfer inefficiency effects on the pn data using the *EPSPATIALCTI* task. We searched for and excluded periods of flaring particle background based on single-event light curves in the 10–15 keV band for the MOS detectors and 10–12 keV band for the pn, using events from the entire detector area in each case. To avoid the effects of pile-up we extracted source spectra from annular regions. To decide on appropriate excision radii we used the *EPATPLOT* task. For MOS1 and MOS2 we extracted source spectra from annuli with inner and outer radii of 7.5 and 50 arcsec; background spectra were extracted from source-free circular regions of radius 100 arcsec located on the same chip as the source. For pn we extracted source counts from an annulus between 10 and 40 arcsec; background counts were extracted from a nearby chip, using a source-free 110×110 arcsec 2 rectangular region at a similar distance from the read-out node as the source. We used standard event selection criteria. After creating response files with *RMFGEN* and *ARFGEN* we grouped the spectra in the 0.3–10 keV range with the *SPECGROUP* task, imposing a minimum signal-to-noise ratio of 5, and limiting oversampling of the energy resolutions of the detectors to a maximum factor of 2.

We analysed the *NuSTAR* (Harrison et al. 2013) data (ObsID 30001004002) using the *NuSTAR* Data Analysis Software (*NUSTARDAS*), version 1.4.1, in conjunction with the *NuSTAR* calibration data base, version 20140715. We reprocessed the raw data using *NUPIPELINE*, and then extracted source spectra and created response files for both (FPMA and FPMB) detectors with the *NUPRODUCTS* task. The source spectra were extracted from circular regions of radius 75 arcsec centred on the source. Because of the significant variation of the background across the two detectors, we modelled the background contribution in the source extraction regions with the *NUSKYBGD* tools package (Wik et al. 2014). We grouped the spectra in the 3–78 keV band, requiring a minimum signal-to-noise ratio of 9 per group. This ensured that the energy resolution of the detectors (~ 400 eV below ~ 50 keV) was nowhere oversampled by more than a factor of 2.

We fitted the spectra from the five detectors (*XMM–Newton* EPIC MOS1/MOS2/pn in the 0.3–10 keV band and *NuSTAR* FBMA/FPMB in the 3–78 keV band) simultaneously with XSPEC, version 12.8.2. We initially fitted the spectra with two additive components (one for the soft thermal emission and another for the harder power-law component), modified by absorption. In addition, we included in our model an overall multiplicative factor – fixed to 1 for the pn but free for the other detectors – to account for possible cross-calibration shifts between the detectors. All other parameters were tied between the five detectors. We used the TBABS absorption model with WILM abundances (Wilms, Allen & McCray 2000) and VERN cross-sections (Verner et al. 1996). We modelled the soft component with the NSATMOS neutron star atmosphere model (Heinke et al. 2006), fixing the neutron star mass at $1.4 M_{\odot}$, the distance at 1.2 kpc, and the fraction of the surface emitting at 1, but allowing the effective surface temperature and the radius of the neutron star to vary. Trying a fit with a simple power law for the hard component [i.e. $\text{CONST}^*\text{TBABS}^*(\text{NSATMOS}+\text{POWERLAW})$] we found poor agreement with the data, with systematic residuals at the higher energies indicating the presence of a break in the power law, as reported by Chakrabarty et al. (2014). We also found that replacing the simple power law with a broken power law (BKNPOWER), a cut-off power law (CUTOFFPL), or a thermal bremsstrahlung model (BREMSS) provided a significantly better fit for the hard component, again in agreement with Chakrabarty et al. (2014). In Section 4.3 we describe how we used these better-fitting two-component models as a basis for placing limits on the possible presence of a second hard component in the 0.3–78 keV spectrum.

3.2 Search for pulsations from Cen X-4

If the magnetosphere is strong enough to truncate the disc and drive a propeller or form a trapped disc, it is also strong enough to channel the accretion flow on to the magnetic poles of the star, potentially resulting in pulsed emission (as long as some material hits the stellar surface; see Section 2.2.1). If the emission arises entirely from the surface of the star, any rotational asymmetry in accretion on to the star should be detectable, since the accretion flow itself is invisible. No pulsations have ever been detected in Cen X-4, but recent advances in pulse search techniques (Messenger 2011; Pletsch et al. 2012) have made it possible to search for high-frequency pulsations from very low luminosity sources. In this spirit we have undertaken a systematic search for pulsations in quiescent data from Cen X-4 using a semicoherent search strategy (Messenger 2011).

Cen X-4 was observed in quiescence with *XMM–Newton* on 2003 March 1 (MJD 52699) for a total on-source exposure time of ~ 80 ks. The EPIC pn detector operated in timing mode (with the thin filter), recording data with a sampling time of 29.56 μs . Since we searched spin periods down to the millisecond range, we selected only data coming from the pn detector.

The data were processed using SAS, version 13.0.0, with the most up-to-date calibration files available when the reduction was performed (2014 May). The photons were filtered by applying standard screening criteria and by removing solar flares and telemetry dropouts. After filtering, the total net exposure time was 68.5 ks.

To look for X-ray pulsations we adopted a semicoherent search strategy (Messenger 2011). We define fully coherent searches as those in which the phase of a matched filter tracks that of the signal for the duration of the observation. For long observations and large parameter spaces such searches rapidly become computationally unfeasible. For finite computational power the most sensitive

Table 1. Parameter space boundaries for the Cen X-4 search.

Parameter	Units	Min	Max
ν	Hz	50	1500
a_1	lt s	0.04	1.9
P_b	s	54 000	54 720
T_{asc}	s	Full orbit	

Note. ν is the spin frequency; a_1 is the projected semimajor axis of the neutron star orbit; P_b is the orbital period; and T_{asc} is the time of passage through the ascending node (corresponding to the point at 0° true longitude).

searches are semicoherent (Prix & Shaltev 2012). In a semicoherent search the data are divided into short segments of length ΔT , and each segment is searched *coherently*. The different segments are then combined incoherently. This is done in such a way as to ensure that signal parameters are consistent between data products combined from different segments, but does not impose signal phase consistency at the segment boundaries. An extensive description of the technique can be found in Messenger (2011) and in Messenger & Patruno (2014) where the same scheme has been adopted to search for pulsations in the LMXB Aql X-1.

During the search we assumed a circular orbit and no prior knowledge of the orbital phase, while we restricted the orbital period and semimajor axis according to the values reported in Chevalier et al. (1989) (see also Table 1). To avoid the influence of possible unreported systematics we extended the range of values used for the orbital period. While the search is sensitive to signals with time-varying amplitude (on time-scales $> \Delta T$), for the purposes of our reported sensitivity we assume a constant fractional amplitude of the pulsations for the entire duration of the observation.

The data were divided into 443 segments of $\Delta T = 128$ s that were each searched coherently. A cubic grid of templates using a 10 per cent worst-case mismatch was then placed on the two-dimensional parameter space⁴ of the spin and spin derivative. To combine the data products from each segment an additional bank of random templates was then used to cover the space defined by the Cartesian product of the physical parameter ranges given in Table 1. This bank was constructed so as to provide a 90 per cent coverage at 10 per cent mismatch, and consequently contains 3.42×10^{10} trials.

Our expected theoretical sensitivity is 6.8 per cent rms, adopting a multitrail false-alarm rate of 1 per cent (conservatively assuming that our trials are independent) and a 10 per cent false dismissal probability. We detected no significant pulsations with a fractional amplitude upper limit of 6.4 per cent.

4 THE ORIGIN OF THE QUIESCENT CEN X-4 SPECTRUM

What is the origin of the power-law component in the quiescent X-ray spectrum of Cen X-4? While the soft component is well described by quasi-thermal emission from the entire neutron star surface (Rutledge et al. 1999; Cackett et al. 2010), the origin of the power law is unclear. Its luminosity clearly comes from

⁴ Within each segment the signal was approximated by its second-order Taylor expansion in phase. The choice of maximum expansion coefficient is dictated by the choice of fixed segment length (see Messenger 2011).

accretion energy, but the dominant radiation mechanism, geometry, and location of the emission are uncertain. As we show below, the low-energy spectral cut-off and hard spectral index clearly suggest bremsstrahlung emission (as previously concluded by Chakrabarty et al. 2014), while the near-balance between the thermal and power-law components strongly suggests the power law is emitted from the boundary layer of the star, rather than in the accretion flow.

4.1 Emission from the accretion flow

4.1.1 Constraining radiation from a radiatively inefficient flow

Chakrabarty et al. (2014) interpret the power-law X-ray spectral component of Cen X-4 as an ADIOS flow – a radiatively inefficient flow model proposed by Blandford & Begelman (1999). In this model, the inner 10^3 – $10^5 R_S$ of the accretion flow no longer forms a thin disc, and instead gravitational potential energy released by infall is primarily advected outwards, launching a strong wind from the outer part of the accretion flow. As a result the net accretion rate in this region becomes a strong function of radius:

$$\dot{M}(r) = \dot{M}(r_{\text{in}}) \left(\frac{r}{r_{\text{in}}} \right)^p, \quad (7)$$

where $0 \leq p < 1$ is a scaling parameter for the local accretion rate as a function of radius: $p = 0$ gives the standard solution (with no outflow), while $p < 1$ is imposed so that the amount of gravitational energy released increases with decreasing radius. The accretion rate through the flow can thus vary by several orders of magnitude between the inner and outer edges of the ADIOS flow, r_{in} and r_{out} .

Fitting the hard X-ray spectrum with a thermal bremsstrahlung model, Chakrabarty et al. (2014) find a gas temperature of 18 keV. In their interpretation of the spectrum, they assume the entire accretion flow has this temperature and use the observed luminosity to infer a density profile for the ADIOS flow. They assume that the total luminosity from the source corresponds to the net accretion rate on to the star at $r_{\text{in}} \sim R_*$ (see equation 1) so that $\dot{M} \simeq 4 \times 10^{-6} \dot{M}_{\text{Edd}}$. They adopt a thick toroidal geometry for the flow with a radial velocity $v_r = \mu \sqrt{GM_*/r}$ (where $\mu \simeq 0.1$), meaning that the infall velocity is a considerable fraction of the Keplerian velocity. The hardness of the spectral index and low energy of the spectral cut-off exclude synchrotron emission and inverse Compton scattering as plausible emission mechanisms, and Chakrabarty et al. (2014) conclude that the hard X-rays are most likely produced by bremsstrahlung emission. They estimate $p > 0.8$ –1 for the accretion rate as a function of radius.

Overall, this interpretation presents several difficulties in explaining the behaviour of Cen X-4. First, it essentially assumes that the flow is radiatively efficient: the amount of luminosity in the flow is roughly equal to the net accretion rate at r_{in} . The radiative efficiency of an ADIOS flow is not defined a priori, and is so high in the present case because there is so much hot gas in the outer parts of the flow. With a temperature of 18 keV, the gas around r_{out} has a sound speed, c_s , equal to or considerably greater than the Keplerian velocity of the flow, v_K (and considerably larger than the virial velocity, about $0.4 v_K$; Narayan & Yi 1995). In contrast, the Blandford & Begelman (1999) model predicts a sound speed of at most $c_s \sim 0.6$ – $0.8 v_K$. This mismatch is only exacerbated by the observation that the spectral index decreases at lower luminosities (Cackett et al. 2010; Chakrabarty et al. 2014), which Chakrabarty et al. (2014) interpret as evidence of an increased gas temperature with decreasing \dot{M} .

As mentioned previously, if the power-law component is emitted by the accretion flow, the approximately equal contribution of the thermal and power-law components of the spectrum is not naturally explainable, nor are the short time-scales on which they covary. As presented in Blandford & Begelman (1999), and recently revisited by Begelman (2012), the ADIOS flow can be extremely radiatively inefficient (i.e. adiabatic): the amount of radiation from the flow can be arbitrarily small, since most of the accretion energy is used to launch an outflow. The observed balance between the thermal and power-law components would therefore be coincidental. The large geometric separation between the thermal component (at R_*) and power-law component (at $\sim 10^4 R_*$) is also difficult to reconcile with the rapid observed variability. At $10^4 R_*$ the characteristic accretion time, $t_{\text{visc}} \sim r/v_r = \mu^{-1} \sqrt{r^3/GM_*}$, is about 770 s, or nearly an order of magnitude larger than the shortest observed time-scale for covariation of the two spectral components (Campana et al. 2004; Cackett et al. 2010; Chakrabarty et al. 2014).

The considerable uncertainty in the accretion rate at r_{in} can alleviate the energetic difficulties of the proposed ADIOS solution. Cen X-4 could be in a strong propeller state, so that most of the accretion flow is expelled by the magnetic field when it reaches r_m (although as we argue in Section 2.2 the lack of detected pulsations makes this seem unlikely). The strength of the thermal component is set by residual gas accreting on to the star, which could then be much lower than the accretion rate in the inner part of the accretion flow. If the accretion rate in the flow is considerably higher and most of the gas is expelled in a propeller outflow, the gas density and temperature will be higher, so that a weaker outflow and smaller ADIOS region will produce the observed emission. However, if there is a strong propeller the covariation of the thermal and power-law components and their near balance is hard to understand, since now a strong propeller will further break the connection between accretion flow and the surface of the star. Although the ADIOS model (and other radiatively inefficient accretion flows) can qualitatively explain the observed power-law emission from Cen X-4, we conclude that the model is implausible in detail.

4.1.2 Emission from a radiatively efficient flow?

Simple physical arguments can also be used to show that the emission cannot be produced by a radiatively efficient flow in the inner part of the flow. A geometrically thin, optically thin hot accretion flow is unstable to expansion since it cannot cool radiatively as fast as it is heated by turbulence (Frank et al. 2002). This expansion implies that at the low observed accretion rates the gas density would not be high enough to produce the observed spectrum from bremsstrahlung (which would require a very small disc scale height). In black holes at somewhat higher accretion rates, it has been suggested that the hard X-ray emission comes from an optically thin corona overlying a cold, optically thick disc, although in this case the underlying disc is heated and should produce comparable luminosity to the corona (Haardt & Maraschi 1991) and a strong Fe K emission line (e.g. Ross & Fabian 1993), neither of which are observed. Since roughly 50 per cent of the emission is coming from the surface, the energy balance between the hard and soft component is not accounted for: the underlying disc should be as luminous as the corona, and the blackbody component (made up of a disc and the surface) should clearly dominate over the power-law one.

A simple energy balance calculation shows that the emission cannot come from inverse Compton scattering of a large optical depth corona above a thin disc. Chakrabarty et al. (2014) fit the

power-law component with an inverse Compton spectrum from a disc, and find $\tau \sim 4$ and $kT \sim 6$ keV. The scale height of such a corona is

$$H = \left(\frac{kTr}{m_p GM_*} \right)^{0.5} r \sim 0.01r, \quad (8)$$

which implies a scale height of about 10^4 cm in the inner parts of the flow.

For an electron-scattering optical depth of $\tau = \sigma_T n_e H \sim 4$ (assuming ionized hydrogen gas), the surface density of the corona will be

$$H n_e \simeq 6 \times 10^{24} \text{ cm}^{-2}. \quad (9)$$

This implies a number density of $n_e \sim 6 \times 10^{20} \text{ cm}^{-3}$ in the inner accretion flow, which is too high for the heating rate (from turbulent viscosity) to balance radiative losses from bremsstrahlung at the observed gas temperature, as a simple calculation shows. Assuming $\dot{M} = 8.1 \times 10^{12} \text{ g s}^{-1}$ (from the observed luminosity), the local heating rate in the inner disc will be $\sim 3GM_*\dot{M}/(8\pi R_*^3) \sim 9.6 \times 10^{19} \text{ erg s}^{-1} \text{ cm}^{-2}$ (Frank et al. 2002). The frequency-integrated bremsstrahlung emission function ($\text{erg s}^{-1} \text{ cm}^{-3}$) for ionized gas of density n_e and temperature T_e is (assuming ionized hydrogen and a Gaunt factor of 1.2; Rybicki & Lightman 1979)

$$U_{\text{brems}} = 1.7 \times 10^{-27} n_e^2 T_e^{1/2}. \quad (10)$$

The emission rate per unit area of the corona (integrated over the scale height of 10^4 cm) will thus be $\sim 3 \times 10^{23} \text{ erg s}^{-1} \text{ cm}^{-2}$ which is much larger than the energy released in turbulent processes.

There is thus no obvious way for an accretion flow (radiatively efficient or not) at such a low accretion rate to produce the (apparent) bremsstrahlung emission unless the accretion rate at the inner edge is considerably larger than implied by the observed emission. This requires a strong propeller, which then does not explain the apparent balance between the thermal and power-law components, nor the observed covariation of the two components on short time-scales.

4.2 Emission from a boundary layer

Given that more than half the emission in Cen X-4 comes from a quasi-blackbody component mostly generated by accretion, and that the two spectral components are roughly equal and covary, the power-law component could also plausibly originate close to the neutron star surface.⁵ As discussed in Section 2, a large fraction (at least 1/4–1/2) of the total accretion energy is released in the boundary layer of the star, in the final impact of gas on to the stellar surface. Although it is not clear how the gas's kinetic energy is converted to radiation in the boundary layer, it is reasonable to assume that not all the radiation will come from an optically thick layer and there may be a strong power-law contribution.

The most plausible radiation mechanism to explain the power-law spectrum is optically thin thermal bremsstrahlung. The joint *XMM-Newton* and *NuSTAR* fit of Chakrabarty et al. (2014) suggests the bremsstrahlung component has a luminosity of $L_X \simeq 7.2 \times 10^{32} \text{ erg s}^{-1}$ (0.3–78 keV, assuming a distance of 1.2 kpc) and temperature of $kT_e \simeq 18$ keV for the bremsstrahlung component. The total inferred luminosity from 0.3 to 78 keV is $1.5 \times 10^{33} \text{ erg s}^{-1}$. Inverse Compton scattering from a surface

⁵ In the refereed version of their work, Chakrabarty et al. (2014) have independently suggested the same possibility, and reach similar conclusions to ours as to the nature of the boundary layer.

corona is excluded, since if the optical depth were high enough to produce the emission it would completely obscure the (thermal) surface emission from the star. Synchrotron emission may also be important if the boundary layer has magnetic turbulence with $\beta = P_{\text{gas}}/P_B \sim 1$, but again the low cut-off energy is inconsistent with emission arising from power-law electrons accelerated by shocks (which in general has a much higher cut-off energy). A model which produces synchrotron emission from the interaction of a pulsar radio jet with the outer accretion disc (suggested by Campana et al. 2004) is carefully considered and disfavoured in Chakrabarty et al. (2014).

If the boundary layer covers the entire surface of the star with a scale height b and emits bremsstrahlung radiation, the amount of bremsstrahlung radiation and its temperature (inferred from the strength and cut-off energy of the X-ray spectral power-law component) can be used to relate the mean density and scale height of the boundary layer:

$$\begin{aligned} L_{\text{brems}} &= U_{\text{brems}} 4\pi R_*^2 b \\ &= 3.1 \times 10^{-10} n_e^2 b \left(\frac{kT_e}{18 \text{ keV}} \right)^{1/2} \left(\frac{R_*}{10^6 \text{ cm}} \right)^2. \end{aligned} \quad (11)$$

Thus,

$$\begin{aligned} n_e^2 b &= 2.3 \times 10^{42} \left(\frac{R_*}{10^6 \text{ cm}} \right)^{-2} \\ &\times \left(\frac{L_{\text{brems}}}{7.2 \times 10^{32} \text{ erg s}^{-1}} \right) \left(\frac{kT_e}{18 \text{ keV}} \right)^{-1/2} \text{ cm}^{-5}. \end{aligned} \quad (12)$$

We can set an upper limit on the density of the boundary layer by considering the accretion rate required for the gravitational potential energy released to match the observed luminosity. Assuming the entire luminosity (L_{tot}) comes from the boundary layer, the accretion rate on to the star will be

$$\dot{M} = \frac{L_{\text{tot}}}{v_{K,*}^2 \mathcal{F}_{\text{bl}}}, \quad (13)$$

where $v_{K,*} \equiv (GM_* R_*^{-1})^{1/2}$ is the Keplerian velocity at R_* and \mathcal{F}_{bl} is the fraction of gravitational potential energy released in the boundary layer.

The accretion rate on to the star will be

$$\dot{M} = 4\pi R_*^2 m_p n_e v_{R,*}, \quad (14)$$

where $v_{R,*}$ is the radial infall velocity in the boundary layer. Combining equations (14) and (13) gives the characteristic number density in the boundary layer:

$$\begin{aligned} n_e &= 7.7 \times 10^{23} \left(\frac{L_{\text{tot}}}{1.5 \times 10^{33} \text{ erg s}^{-1}} \right) \left(\frac{\mathcal{F}_{\text{bl}}}{0.5} \right)^{-1} \\ &\times \left(\frac{M_*}{1.4 M_\odot} \right)^{-1} \left(\frac{R_*}{10^6 \text{ cm}} \right)^{-1} v_{R,*}^{-1} \text{ cm}^{-3}. \end{aligned} \quad (15)$$

The boundary layer (assuming there is no magnetosphere) is expected to be strongly turbulent, since infalling gas must transition from roughly Keplerian orbits to corotation with the star. Shakura & Sunyaev (1988) derived some simple physical properties of the boundary layer, assuming that a turbulent flow develops. The net infall velocity of the gas can be expressed as

$$v_{R,*} \simeq v_{K,*} \frac{\mathcal{M}^2 (3 + \Omega_*/\Omega_{K,*}) b}{2C R_*}, \quad (16)$$

where \mathcal{M} is the Mach number of the flow, $\Omega_*/\Omega_{K,*}$ is the ratio of the stellar spin frequency to the Keplerian frequency at the surface

of the star, and C is a numerical factor of order unity (representing uncertainty in the nature of the turbulence). If we assume strong, nearly supersonic turbulence with $\mathcal{M} \sim 1$, the maximum infall velocity will be

$$v_{R,*} \sim \frac{3}{2} \frac{b}{R_*} v_{K,*}. \quad (17)$$

This sets an upper limit on $n_e b$,

$$n_e b > 3.8 \times 10^{19} \left(\frac{R_*}{10^6 \text{ cm}} \right)^{1/2}. \quad (18)$$

From equation (12) we thus get an upper limit on the number density of the boundary layer:

$$n_e < 6 \times 10^{23} \text{ cm}^{-3}. \quad (19)$$

We can also infer a hydrostatic scale height for the corona. For a coronal temperature of 18 keV (corresponding to a sound speed $c_s = \sqrt{kT/m_p} \simeq 1.3 \times 10^8 \text{ cm s}^{-1}$) the scale height will be

$$b \sim R_* \left(\frac{c_s}{v_{K,*}} \right)^2 \sim 10^2 \text{ cm}, \quad (20)$$

which is consistent with the limits we have derived and implies a number density of $n_e \sim 6 \times 10^{19} \text{ cm}^{-3}$ (note that this implies a Compton optical depth $\tau \sim \sigma_T n_e b < 10^{-2}$, so that electron scattering will essentially be irrelevant).

This solution assumes that the boundary layer is a single-temperature gas. This will be true as long as the density is high enough for the ions and electrons to maintain collisional equilibrium faster than the ions can heat (via turbulence) or the electrons can cool by radiating. As a final check on our solution above, we can compare the predicted turbulent heating time-scale (the infall time), the cooling time-scale (bremsstrahlung emission from electrons), and the time-scale for the electrons and ions to reach collisional equilibrium.

The characteristic heating time for the gas is approximately the infall time:

$$t_{\text{heat}} \simeq \frac{b}{v_{R,*}} \simeq \Omega_{K,*}^{-1} = 7.3 \times 10^{-5} \text{ s}, \quad (21)$$

while the time-scale for the gas to cool via bremsstrahlung emission will be (e.g. King & Lasota 1987)

$$\begin{aligned} t_{\text{brems}} &\simeq 2 \times 10^{11} n_e^{-1} T_e^{1/2} \\ &= 5.7 \times 10^{-5} \left(\frac{n_e}{6 \times 10^{19} \text{ cm}^{-3}} \right)^{-1} \left(\frac{kT_e}{18 \text{ keV}} \right)^{1/2} \text{ s}. \end{aligned} \quad (22)$$

The time-scale for electrons and ions to reach equilibrium will be (Boyd & Sanderson 1969)

$$t_{e-i} = 27.5 T_e^{3/2} n_e^{-1} \left(1 + \frac{1}{\xi} \right), \quad (23)$$

where $\xi \equiv (T_i - T_e)/T_e$ is the fractional difference between the ion and electron temperatures. For $n_e \sim 6 \times 10^{19} \text{ cm}^{-3}$, and the inferred gas temperature, 18 keV, $t_{e-i} \sim t_{\text{heat}}$ even for a significantly two-temperature plasma:

$$\begin{aligned} t_{e-i} &< 1.4 \times 10^{-6} \left(1 + \frac{1}{\xi} \right) \left(\frac{n_e}{6 \times 10^{19} \text{ cm}^{-3}} \right)^{-1} \\ &\quad \times \left(\frac{kT_e}{18 \text{ keV}} \right)^{3/2} \text{ s}. \end{aligned} \quad (24)$$

Furthermore, for a small boundary layer scale height, the radiative cooling time is significantly longer than the cooling time

from expansion:

$$\begin{aligned} t_{\text{exp}} &\sim \frac{b}{c_s} \\ &\simeq 8 \times 10^{-7} \left(\frac{b}{10^2 \text{ cm}} \right) \left(\frac{kT_e}{18 \text{ keV}} \right)^{-1/2} \text{ s}. \end{aligned} \quad (25)$$

The coronal layer may therefore expand into a two-temperature plasma with a significantly larger scale height than $b \sim 10^2 \text{ cm}$, but a more detailed energy balance is needed to explore the coronal structure in more depth. Regardless of this uncertainty, the basic model for bremsstrahlung from a surface corona fits the observed spectrum for a reasonable range of scale heights and densities and satisfies basic energy balance requirements. It also offers a reasonable explanation for the energy balance between the bremsstrahlung and blackbody components.

4.3 How radiatively inefficient is the accretion flow?

The quiescent X-ray spectrum of Cen X-4 is most likely produced by the final fall of accreting matter on to the surface of the neutron star. The accretion flow itself (which should radiate about half the total liberated gravitational energy if the flow is efficiently radiating; Section 2) is not detected, and we can constrain its intrinsic radiative efficiency from setting upper limits on the presence of a second hard X-ray component (with luminosity L_{flow}) in the observed X-ray spectrum. From the upper limit on L_{flow} we can use the limits on the energy available to be radiated from each component obtained in Section 2 to set upper limits on the intrinsic radiative efficiency of the accretion flow, assuming it radiates primarily in X-rays.

To estimate a rough upper limit on the possible flux from the accretion flow we added a third emission component to the three better-fitting two-component models discussed in Section 3.1 (i.e. the ones where the hard component was modelled by a broken power law, a cut-off power law, or a thermal bremsstrahlung model). We initially used a simple (unbroken) power law (PEGWRLW) for this extra component, since this model has only two parameters (a slope and normalization), and since power-law emission is typically seen in the accretion flow of both black hole and neutron star binaries at low luminosities. We defined the normalization of this additional power-law component to be its unabsorbed flux in the 0.3–78 keV band (i.e. the combined *XMM-Newton* and *NuSTAR* range). For a given fixed photon index we then derived a 95 per cent confidence upper limit on this power-law flux (using $\Delta\chi^2 = 2.706$) and converted this upper flux limit to an upper limit on the fractional contribution of the power-law component to the total 0.3–78 keV unabsorbed flux. We explored the range 1.0–2.5 for the photon index of the additional power law. We carried out this procedure for each of the three original hard-component models (BKNPOWER, CUTOFFPL, and BREMSS). In the specific cases of the broken power law and cut-off power law we constrained the values of the photon indices of those components to be ≥ 1.0 to prevent the indices from assuming unphysically low values during the upper limit calculation.

The procedure described above yielded 95 per cent upper limits on the fractional contribution of the extra power-law component to the total unabsorbed 0.3–78 keV flux in the ranges ~ 0.11 – 0.34 , 0.06 – 0.33 , and 0.06 – 0.26 , for the models with a broken power law, a cut-off power law, and thermal bremsstrahlung, respectively, when varying the photon index of the additional power law between 1.0 and 2.5. In all three cases the highest upper limits were obtained when the photon index of the extra power law was in the range ~ 1.5 – 1.7 . We also repeated our analysis with the neutron star mass

fixed at $1.9 M_{\odot}$ (the value used by Chakrabarty et al. 2014) instead of $1.4 M_{\odot}$, but found that this change had a negligible effect on our results.

The exact shape of a possible extra spectral component arising from the accretion flow itself is uncertain; e.g. it is possible that rather than being a simple power law throughout the 0.3–78 keV range there could be a low- and/or high-energy roll-over present that affects the emission in the observed bandpass. Therefore, to make the analysis more robust, we repeated our analysis procedure with the simple power law replaced by the `NTHCOMP` Comptonization model (Zdziarski, Johnson & Magdziarz 1996; Życki, Done & Smith 1999). We explored a range of values for three of the model parameters. For the seed photon temperature (governing the low-energy roll-over) we explored the range 0.2–1.0 keV; for the electron temperature (governing the high-energy roll-over) we considered values of 5–300 keV; and for the asymptotic power-law photon index (set by the optical depth of the Comptonizing plasma as well as the electron temperature) we considered the range 1.1–2.5. The seed photon distribution was assumed to have a blackbody shape. Unsurprisingly, it was possible to find combinations of parameter values that allowed a somewhat larger contribution from this component than was the case for a simple power law; on the fractional contribution of the `NTHCOMP` component to the total unabsorbed 0.3–78 keV flux we find 95 per cent upper limits that range from ~ 0.03 to as much as ~ 0.46 .

For the largest fractional contributions, however, the additional `NTHCOMP` component essentially replaces the original hard component with one that is physically implausible. The `NTHCOMP` component in these cases has a seed photon temperature of ~ 0.7 –1 keV and a typical photon index of ~ 1.9 –2.0. The fractional contribution of the component is virtually independent of the upscattering electron temperature (which determines the hard X-ray shape of the spectrum), indicating that the contribution to the soft X-rays is what chiefly limits the weight of the additional component. In this fit, the X-ray spectrum up to the high-energy roll-over is essentially fitted by the peak of the blackbody seed photon distribution with some upscattered photons, while the observed break is reproduced by the steeper power-law tail of the Comptonized photon distribution. There is no independent indication or theoretical expectation for such a hard X-ray seed photon population, so the addition of a more complex model mainly serves to demonstrate that the detailed shape of an additional component in the hard X-rays does not significantly influence how strong the contribution of such a component could be. We thus use the limits given by the addition of the simpler model (a power law) to set limits on the intrinsic radiative efficiency of the accretion flow.

We conclude that the luminosity of the accretion flow itself, L_{flow} , can make up no more than ~ 6 –34 per cent of the total X-ray luminosity, and an even smaller fraction of the total luminosity, given the significant observed UV flux. Since the UV contribution and origin are still unclear, however, we do not include it in our estimate of $L_{\text{flow}}/L_{\text{tot}}$.

The luminosity of a given spectral component will be

$$L = \dot{E}_{\text{pot}} \mathcal{F} \varepsilon, \quad (26)$$

where ε is the intrinsic radiative efficiency of the component (i.e. the fraction of the gravitational potential energy available to it that the component radiates away). The system's total luminosity will then be

$$L_{\text{tot}} = L_{\text{flow}} + L_{\text{bl}} = \dot{E}_{\text{pot}} (\mathcal{F}_{\text{flow}} \varepsilon_{\text{flow}} + \mathcal{F}_{\text{bl}} \varepsilon_{\text{bl}}). \quad (27)$$

By measuring L_{tot} , assuming $\varepsilon_{\text{bl}} = 1$ (the boundary layer radiates energy efficiently), and using our upper limits on L_{flow} (see above) we can estimate $\varepsilon_{\text{flow}}$, provided we can constrain \mathcal{F}_{bl} and $\mathcal{F}_{\text{flow}}$. As described in Section 2, this will depend on the neutron star's spin, size, and magnetic field, as well as the width of the boundary layer. Since the gravitational potential energy liberated by the different components can be unequal, i.e. the intrinsic efficiency can still be high if there is very little energy available to be radiated in the flow compared with the disc (as in e.g. a trapped disc scenario). The intrinsic radiative efficiency of the accretion flow is then

$$\varepsilon_{\text{flow}} = \frac{\mathcal{F}_{\text{bl}} L_{\text{flow}}}{\mathcal{F}_{\text{flow}} L_{\text{bl}}} = \frac{\mathcal{F}_{\text{bl}}}{\mathcal{F}_{\text{flow}}} \left(\frac{L_{\text{flow}}/L_{\text{tot}}}{1 - L_{\text{flow}}/L_{\text{tot}}} \right). \quad (28)$$

For our observed range of upper limits on L_{flow} , this gives $\varepsilon_{\text{flow}} < 0.06$ –0.5 if $\mathcal{F}_{\text{bl}} = \mathcal{F}_{\text{flow}}$. If none of the factors below plays a significant role, this demonstrates that the flow is intrinsically radiatively inefficient. As elsewhere in the paper, we assume that the boundary layer is radially narrow ($b \ll R_*$), based on the reasoning presented at the beginning of Section 2.

The size, spin, and magnetic field of Cen X-4 are all unknown. However, the absence of pulsations and presence of Type I X-ray bursts suggests a relatively weak magnetic field (we adopt 10^8 G as a fiducial magnetic field for the calculations below), while the large observed outbursts (and hence high mass transfer rates) suggest a large amount of spin-up and a fast spin period, so we adopt 2 ms as a fiducial spin period.

From Section 2, very small (soft equation of state) slowly rotating neutron stars (over a range of mass) can have $\max(\mathcal{F}_{\text{bl}}/\mathcal{F}_{\text{flow}}) \sim 1.8$ –2, which corresponds to a radiative efficiency $\varepsilon_{\text{flow}} < 0.1$ –1 (considering the range of upper limits on L_{flow}).

Alternatively, if the star is rapidly rotating without a large magnetosphere (the most likely scenario, given the lack of any indication of a magnetic field) the boundary layer will be dimmer than the accretion flow, and $\mathcal{F}_{\text{bl}}/\mathcal{F}_{\text{flow}} \sim 0.4$ –0.6, which will correspond to a smaller intrinsic efficiency for the flow: $\varepsilon_{\text{flow}} < 0.03$ –0.3.

If a magnetic field does regulate the flow near the star the two scenarios presented in Section 2.2 give significantly different predictions for $\varepsilon_{\text{flow}}$. Using the propeller and trapped disc models presented in Fig. 2 we can estimate \dot{M} , \mathcal{F}_{bl} , and $\mathcal{F}_{\text{flow}}$ that correspond to the observed luminosity, $L_X \simeq 9 \times 10^{-6} L_{\text{Edd}}$.

If a strong propeller is operating, the observed boundary layer luminosity corresponds to an accretion rate of $\dot{M} = 1.4 \times 10^{-4} \dot{M}_{\text{Edd}}$, with $\mathcal{F}_{\text{bl}} = 0.04$ (using the fit to the MHD simulations of Ustyugova et al. 2006). The corresponding energy release in the accretion flow is $\mathcal{F}_{\text{flow}} = 0.09$. This corresponds to a very small intrinsic efficiency for the flow, $\varepsilon_{\text{flow}} < 0.03$ –0.2.

Alternatively, if a trapped disc forms, the flow is truncated close to the magnetospheric radius (around 30 km) and is thus much less luminous than the boundary layer: $\mathcal{F}_{\text{flow}} \simeq 0.17 \mathcal{F}_{\text{bl}}$. In this case the intrinsic radiative efficiency of the accretion flow is difficult to constrain, and we find $\varepsilon_{\text{flow}} \sim 0.4$ –1 as an upper limit. Note that the ‘trapped disc’ presented here is an extreme limiting case: in reality there may be some outflow (even substantial) where the flow hits the magnetic field. As long as there is considerable angular momentum from the star transported through the inner radius of the flow, the disc will stay trapped and r_{in} will remain close to r_c . Any outflow of matter in the inner parts of the flow will decrease the radiative efficiency of the boundary layer, and thus require a smaller value for $\varepsilon_{\text{flow}}$.

For most reasonable values of the neutron star spin, size, and magnetic field, the non-detection of an accretion flow component in Cen X-4 thus demonstrates that the flow is intrinsically radiatively

inefficient. Cen X-4 shows no indication of a significant magnetic field (from our pulsation search), so we consider the most likely scenario (based on the known history and properties of the star) to be a rapidly spinning weakly magnetized star. In this case the intrinsic efficiency is $\lesssim 30$ per cent. In the least constraining case (a trapped disc with no magnetically driven outflow) the limits cannot conclusively show a radiatively inefficient flow, but again this case may represent an extreme solution.

The hard X-ray spectrum with a cut-off at ~ 10 keV, the balance between the quasi-blackbody and power-law components and the covariation of the two all strongly suggest that the power-law emission originates close to the star, most likely via accretion on to the surface of the star. By extension, the power-law emission seen in other quiescent neutron star binaries likely has the same origin, and their spectra could be interpreted in the same way. Moreover, an observation during the decay phase of an outburst could allow both the emission from the boundary layer and the accretion flow to be detected simultaneously as power-law components with two different cut-off energies. The hard X-ray sensitivity of *NuSTAR* might be able to detect the cut-off of one component directly, which would allow a direct measurement of the strength of each component, and thus offer better constraints on RIAF models. Repeating the analysis above on a neutron star with a better constrained spin period and magnetic field would allow better limits on \mathcal{F}_{bl} and $\mathcal{F}_{\text{flow}}$, although as our analysis above demonstrates, the main uncertainty in \mathcal{F}_{bl} and $\mathcal{F}_{\text{flow}}$ is for the magnetic case where $r_m > r_c$.

5 DISCUSSION

In this paper we have argued that the quiescent emission from the neutron star Cen X-4 originates predominantly from the impact of the accretion flow on to the surface of the star (most likely without strong modulation by the magnetic field), without an equivalent contribution from the accretion flow. This conclusion has consequences for both the properties of the accretion flow (beyond its intrinsic radiative inefficiency) and the neutron star itself, and suggests future observations that can better constrain the properties of both.

Unless there is a very strong magnetic propeller (disfavoured by the lack of pulsations), the low luminosity of Cen X-4 disfavours a strongly advecting accretion flow (ADAF), since in an ADAF the accretion rate is moderately large ($\sim 10^{-3}$ – $10^{-2} \dot{M}_{\text{Edd}}$) and the majority of the accretion energy is carried on to the central object. This conclusion is the same as was reached by Bernardini et al. (2013) and opposite to that of Menou & McClintock (2001), who interpreted the low surface emission from Cen X-4 as evidence of a strong magnetic propeller. As we have demonstrated in this paper, Cen X-4 shows no evidence for magnetic activity: our pulse search did not find pulsations (with an upper limit of 6.4 per cent pulsed fraction), which are likely to be present if a strong magnetic field is channelling the flow (via episodic accretion, see e.g. Section 2.2.1). A more plausible scenario is that the majority of the gas in the accretion flow does not reach the star, as is proposed by various RIAF models (e.g. Blandford & Begelman 1999; Quataert & Gruzinov 2000; Narayan et al. 2003).

Various RIAF models generally require substantially more gas in the accretion flow than is accreted on to the star, and this gas could obscure the stellar surface if the density is high enough and the orbital inclination angle is high (i.e. the accretion flow is observed close to edge on as in dipping neutron star binary sources; see e.g. Homan 2012 for a list of such systems). Our non-detection of the flow does not set a firm constraint on the density of the accretion

flow, since at such low luminosities even the relatively massive disc predicted by the ADIOS model in Chakrabarty et al. (2014) will be very optically thin to electron scattering ($\tau \sim 10^{-3}$). However, if the orbital inclination is high enough and the scale height of the flow stays roughly constant, the optical depth through the flow should increase with the accretion rate, so that by observing nearby neutron stars in a low state ($\sim 10^{-4}$ – $10^{-3} L_{\text{Edd}}$) we may see the emission from the accretion flow and partly obscured emission from the star. It may thus be possible to detect power-law emission from both the central star and the accretion flow. Since the gas in the flow and the surface could have different temperatures and densities, this could manifest in the hard X-rays as two power-law components: one with a break in the hard X-rays from the spectral cut-off of the surface emission (as observed here) and a second power-law component with a lower intensity extending to higher energies (from the moderately optically thin accretion flow). A firm detection of multiple power-law components would put strong constraints on the radiative efficiency of the flow, since it would constrain the relative intensities of the components.

Thermal radiation from the surface of the star could also be used to constrain the optical depth of the accretion flow. Assuming that the entire surface of the star is radiating (which seems reasonable for sources like Cen X-4, which show no clear magnetic activity), a small inferred radiating area could indicate that a considerable amount of emission from the star is being electron scattered by the accretion flow, thus setting a constraint on the effective optical depth and (where the system's inclination is known) the scale height of the flow. It might also be possible to use changes in the pulsation fraction with changing accretion rate in accreting millisecond X-ray pulsars to constrain the optical depth of the intervening flow. In these systems a decrease in pulsation fraction could imply an increased optical depth of the accretion flow, and be used to constrain the optical depth as a function of luminosity.

Since the present observation of Cen X-4 shows both a thermal and power-law component from the surface of the star, good modelling is vital to understand how accreting matter hits the neutron star surface and releases its energy. As is clear from Section 2, the total lack of a boundary layer model for low-accretion-rate neutron star systems means constraining even the most basic properties of boundary layer is only possible in a very qualitative way. Since RIAFs are generally expected to be geometrically thick, they generically have less specific angular momentum than thin discs, so that the flow could bombard the star on mostly radial orbits. Particle bombardment of the neutron star surface was studied by Zampieri et al. (1995) and Deufel, Dullemond & Spruit (2001), and it was found that particle bombardment leads to efficient thermalization of the accretion energy so that the surface emits energy as a modified blackbody. The work of Deufel et al. (2001) additionally found a power-law component of varying strength, radiating either by bremsstrahlung or inverse Compton scattering.

In contrast, the work of Inogamov & Sunyaev (1999) and Popham & Sunyaev (2001) considered a disc accreting on to a boundary layer (where the gas in the boundary layer must redistribute large quantities of angular momentum in order to settle on to the star) and found that most of the accretion energy is released as power-law radiation from a hot corona around the star. If these models are correct and valid even at the low accretion rates seen in Cen X-4, then the thermal/power-law radiation balance could be a result of the angular momentum distribution from the accretion flow, and could thus be used to put an independent constraint on its scale height. Of course, there may also be radiative coupling between the hot corona and the cool neutron star surface, whereby the accretion energy is

radiated by the corona, which then heats the neutron star's surface. This would require a very low albedo for the neutron star's surface. In a future paper we will investigate some of these questions more thoroughly in light of the quiescent observations of Cen X-4, but more detailed theoretical modelling of the boundary layer structure is clearly warranted.

Understanding how the thermal component is produced in Cen X-4 is also important for observations of neutron star cooling, which track the thermal emission from quiescent neutron stars after an extended outburst and fit them with crustal cooling models. Some of these sources also show a power-law component in quiescence. As we argue in this paper, the power-law component in all quiescent neutron stars is most likely generated very close to the surface of the star, and this accretion on to the surface could result in enhanced quasi-blackbody emission. This extra source of energy may complicate the interpretation of crustal cooling for quiescent neutron stars, since this interpretation assumes that the surface temperature of the neutron star is determined only by the cooling of the crust. The possibility of continued accretion on the cooling neutron star has been briefly discussed by e.g. Wijnands et al. (2004), Cackett et al. (2006), and Fridriksson et al. (2011). A recent study of how the spectra of neutron star LMXBs evolve with decreasing luminosity has also suggested that quiescent neutron star spectra (both the quasi-blackbody and power-law components) are dominated by surface emission (Wijnands et al. 2014).

Does Cen X-4 have a substantial dipolar magnetic field? For a spin period of several milliseconds (like accreting millisecond X-ray pulsars), assuming equation (4) still applies, even a very weak field ($\sim 10^6$ G) will truncate the disc for $\dot{M} \sim 10^{-6} \dot{M}_{\text{Edd}}$ and channel the flow on to the stellar surface. This should most likely produce some periodic modulation, but none is detected down to a level of ~ 6.4 per cent. The 'strong propeller' scenario proposed by Menou & McClintock (2001) required a field of at least 10^9 G, which is about an order of magnitude larger than typically seen in accreting millisecond X-ray pulsars. While it is possible that the magnetic geometry of Cen X-4 is such that pulsations are not seen, the relatively large number of quiescent neutron stars without pulsations suggest that this is unlikely to be the case. If LMXBs really do not have strong dipolar fields, it implies a range of at least nine orders of magnitude in the magnetic field strengths of neutron stars.

6 CONCLUSIONS

In this paper we have directly demonstrated that the accretion flow around the quiescent neutron star binary Cen X-4 is most likely undetected and therefore intrinsically radiatively inefficient. We have argued that the near-balance between thermal and power-law components in the X-ray spectrum, the relatively rapid covariation of these components, and the shape of the power-law component (specifically, its hardness and cut-off around 10 keV) all suggest that the entire X-ray spectrum is generated in a boundary layer close to the star. The accretion flow itself is therefore undetected, down to a level of ~ 6 – 34 per cent of the total observed luminosity, directly demonstrating that the flow is most likely radiatively inefficient (within uncertainties of the neutron star properties), as has been postulated by various theoretical work. We have demonstrated how this can set some (modest) constraints on the radiative inefficiency of the accretion flow, and suggested ways in which observations at somewhat higher luminosities with *NuSTAR* could be used to look for two power-law components (with different cut-off energies) in

the hard X-ray radiation, which would more clearly constrain the radiative efficiency of the flow.

We conclude that there is no evidence of a substantial magnetic field in Cen X-4, based on a lack of detection of pulsations down to 6.4 per cent of the total flux, and therefore agree with the conclusion of Bernardini et al. (2013) that a 'strong magnetocentrifugal propeller' (as proposed by Menou & McClintock 2001) is disfavoured. This would imply a span of at least nine orders of magnitude in the dipolar strength of neutron stars. In the absence of a magnetic propeller, and given the relatively large rate of mass transfer from the companion star, the low luminosity of Cen X-4 strongly favours RIAF models in which the majority of the accreting gas is prevented from reaching the inner regions near the star, and could be expelled in an outflow (ADIOS), recycled outward while remaining gravitationally bound (CDAF), or inhibited by a magnetic field ('magnetically arrested'). We propose using the luminosity versus measured temperature of the blackbody surface component at somewhat higher luminosities to constrain the optical depth of the accretion flow.

We used simple physical arguments for the power-law component to constrain the density of radiating gas: $10^{18} \lesssim n_e \lesssim 10^{23} \text{ cm}^{-3}$. The measured electron temperature and predicted time-scales for heating, cooling, and electron–proton scattering suggest that the plasma likely has a single temperature.

Our conclusion is based on an empirical analysis of the data; a better theoretical understanding of how the accretion energy is released in the boundary layer (and in particular how the thermal component is generated) is necessary to properly understand the implications of our results on how observations of cooling neutron stars should be interpreted, as well as to possibly set additional constraints on the properties of the accreting matter (e.g. its temperature and angular momentum) to further constrain the nature of the RIAF. A more thorough investigation of how accretion flows interact with the surface layers of neutron stars is therefore warranted.

ACKNOWLEDGEMENTS

CRD'A and AP are financially supported by an NWO Vidi grant (PI: Patruno). We are grateful to Daniel Wik for sharing his *NUSKY-BGD* background analysis tools for *NuSTAR*. AP acknowledges very useful conversations with Anne Archibald. CRD'A acknowledges very useful conversations with Deepto Chakrabarty, Marat Gilfanov, Craig Heinke, Andrew King, John Raymond, and Rudy Wijnands.

REFERENCES

- Begelman M. C., 2012, *MNRAS*, 420, 2912
- Bernardini F., Cackett E. M., Brown E. F., D'Angelo C., Degenaar N., Miller J. M., Reynolds M., Wijnands R., 2013, *MNRAS*, 436, 2465
- Bildsten L., 1998, *ApJ*, 501, L89
- Bisnovaty-Kogan G. S., Ruzmaikina A. A., 1974, *Ap&SS*, 28, 45
- Blandford R. D., Begelman M. C., 1999, *MNRAS*, 303, L1
- Boyd T. J. M., Sanderson J. J., 1969, *Plasma Dynamics*. Nelson, London
- Brown E. F., Bildsten L., Rutledge R. E., 1998, *ApJ*, 504, L95
- Cackett E. M., Wijnands R., Linares M., Miller J. M., Homan J., Lewin W. H. G., 2006, *MNRAS*, 372, 479
- Cackett E. M., Brown E. F., Miller J. M., Wijnands R., 2010, *ApJ*, 720, 1325
- Cackett E. M., Brown E. F., Degenaar N., Miller J. M., Reynolds M., Wijnands R., 2013, *MNRAS*, 433, 1362
- Campana S., Stella L., 2000, *ApJ*, 541, 849
- Campana S., Colpi M., Mereghetti S., Stella L., Tavani M., 1998, *A&AR*, 8, 279

- Campana S., Israel G. L., Stella L., Gastaldello F., Mereghetti S., 2004, *ApJ*, 601, 474
- Cardall C. Y., Prakash M., Lattimer J. M., 2001, *ApJ*, 554, 322
- Chakrabarty D. et al., 2014, *ApJ*, 797, 92
- Chevalier C., Ilovaisky S. A., van Paradijs J., Pedersen H., van der Klis M., 1989, *A&A*, 210, 114
- D'Angelo C. R., Spruit H. C., 2010, *MNRAS*, 406, 1208
- D'Angelo C. R., Spruit H. C., 2011, *MNRAS*, 416, 893
- D'Angelo C. R., Spruit H. C., 2012, *MNRAS*, 420, 416
- D'Avanzo P., Campana S., Casares J., Israel G. L., Covino S., Charles P. A., Stella L., 2005, *A&A*, 444, 905
- Deufel B., Dullemond C. P., Spruit H. C., 2001, *A&A*, 377, 955
- Done C., Gierliński M., 2003, *MNRAS*, 342, 1041
- Done C., Gierliński M., Kubota A., 2007, *A&AR*, 15, 1
- Fender R. P., Belloni T. M., Gallo E., 2004, *MNRAS*, 355, 1105
- Frank J., King A., Raine D. J., 2002, *Accretion Power in Astrophysics*. Cambridge Univ. Press, Cambridge
- Fridriksson J. K. et al., 2011, *ApJ*, 736, 162
- Ghez A. M. et al., 2008, *ApJ*, 689, 1044
- Ghosh P., Pethick C. J., Lamb F. K., 1977, *ApJ*, 217, 578
- González Hernández J. I., Reboloto R., Peñarrubia J., Casares J., Israelian G., 2005, *A&A*, 435, 1185
- Grebenev S. A., Sunyaev R. A., 2002, *Astron. Lett.*, 28, 150
- Haardt F., Maraschi L., 1991, *ApJ*, 380, L51
- Harrison F. A. et al., 2013, *ApJ*, 770, 103
- Heinke C. O., Rybicki G. B., Narayan R., Grindlay J. E., 2006, *ApJ*, 644, 1090
- Hessels J. W. T., Ransom S. M., Stairs I. H., Freire P. C. C., Kaspi V. M., Camilo F., 2006, *Science*, 311, 1901
- Homan J., 2012, *ApJ*, 760, L30
- Illarionov A. F., Sunyaev R. A., 1975, *A&A*, 39, 185
- Inogamov N. A., Sunyaev R. A., 1999, *Astron. Lett.*, 25, 269
- Jansen F. et al., 2001, *A&A*, 365, L1
- Jonker P. G., Galloway D. K., McClintock J. E., Buxton M., Garcia M., Murray S., 2004, *MNRAS*, 354, 666
- Kaluzienski L. J., Holt S. S., Swank J. H., 1980, *ApJ*, 241, 779
- King A. R., Lasota J. P., 1987, *A&A*, 185, 155
- Kuulkers E., in't Zand J. J. M., Lasota J. P., 2009, *A&A*, 503, 889
- Lattimer J. M., Prakash M., 2001, *ApJ*, 550, 426
- Lii P. S., Romanova M. M., Ustyugova G. V., Koldoba A. V., Lovelace R. V. E., 2014, *MNRAS*, 441, 86
- Markoff S., Nowak M. A., Wilms J., 2005, *ApJ*, 635, 1203
- Marrone D. P., Moran J. M., Zhao J. H., Rao R., 2007, *ApJ*, 654, L57
- Menou K., McClintock J. E., 2001, *ApJ*, 557, 304
- Menou K., Esin A. A., Narayan R., Garcia M. R., Lasota J. P., McClintock J. E., 1999, *ApJ*, 520, 276
- Messenger C., 2011, *Phys. Rev. D*, 84, 083003
- Messenger C., Patruno A., 2014, *ApJ*, in press
- Narayan R., Popham R., 1993, *Nature*, 362, 820
- Narayan R., Yi I., 1994, *ApJ*, 428, L13
- Narayan R., Yi I., 1995, *ApJ*, 452, 710
- Narayan R., Garcia M. R., McClintock J. E., 1997, *ApJ*, 478, L79
- Narayan R., Igmenshchev I. V., Abramowicz M. A., 2003, *PASJ*, 55, L69
- Paczynski B., 1991, *ApJ*, 370, 597
- Patruno A., Haskell B., D'Angelo C., 2012, *ApJ*, 746, 9
- Pletsch H. J. et al., 2012, *ApJ*, 744, 105
- Popham R., Narayan R., 1991, *ApJ*, 370, 604
- Popham R., Sunyaev R., 2001, *ApJ*, 547, 355
- Pringle J. E., Rees M. J., 1972, *A&A*, 21, 1
- Prix R., Shaltev M., 2012, *Phys. Rev. D*, 85, 084010
- Quataert E., Gruzinov A., 2000, *ApJ*, 539, 809
- Rees M. J., Begelman M. C., Blandford R. D., Phinney E. S., 1982, *Nature*, 295, 17
- Revnitsev M., Gilfanov M., Churazov E., Sunyaev R. A., 1999, *Astrophys. Lett. Commun.*, 38, 121
- Romanova M. M., Ustyugova G. V., Koldoba A. V., Lovelace R. V. E., 2004, *ApJ*, 616, L151
- Ross R. R., Fabian A. C., 1993, *MNRAS*, 261, 74
- Rutledge R. E., Bildsten L., Brown E. F., Pavlov G. G., Zavlin V. E., 1999, *ApJ*, 514, 945
- Rybicki G. B., Lightman A. P., 1979, *Radiative Processes in Astrophysics*. Wiley, New York
- Shakura N. I., Sunyaev R. A., 1973, *A&A*, 24, 337
- Shakura N. I., Sunyaev R. A., 1988, *Adv. Space Res.*, 8, 135
- Sibgatullin N. R., Sunyaev R. A., 1998, *Astron. Lett.*, 24, 774
- Spruit H. C., Taam R. E., 1993, *ApJ*, 402, 593
- Stella L., Campana S., Colpi M., Mereghetti S., Tavani M., 1994, *ApJ*, 423, L47
- Strüder L. et al., 2001, *A&A*, 365, L18
- Sunyaev R. A., Shakura N. I., 1977, *Pis'ma Astron. Zh.*, 3, 262
- Sunyaev R. A., Shakura N. I., 1986, *SvA*, 12, 117
- Torres M. A. P., Casares J., Martínez-Pais I. G., Charles P. A., 2002, *MNRAS*, 334, 233
- Turner M. J. L. et al., 2001, *A&A*, 365, L27
- Ustyugova G. V., Koldoba A. V., Romanova M. M., Lovelace R. V. E., 2006, *ApJ*, 646, 304
- Verner D. A., Ferland G. J., Korista K. T., Yakovlev D. G., 1996, *ApJ*, 465, 487
- Wang Q. D. et al., 2013, *Science*, 341, 981
- Wijnands R., Homan J., Miller J. M., Lewin W. H. G., 2004, *ApJ*, 606, L61
- Wijnands R., Degenaar N., Armas Padilla M., Altamirano D., Cavecchi Y., Linares M., Bahramian A., Heinke C. O., 2014, *MNRAS*, submitted ([arXiv:1409.6265](https://arxiv.org/abs/1409.6265))
- Wik D. R. et al., 2014, *ApJ*, 792, 48
- Wilms J., Allen A., McCray R., 2000, *ApJ*, 542, 914
- Zampieri L., Turolla R., Zane S., Treves A., 1995, *ApJ*, 439, 849
- Zdziarski A. A., Johnson W. N., Magdziarz P., 1996, *MNRAS*, 283, 193
- Życki P. T., Done C., Smith D. A., 1999, *MNRAS*, 309, 561

This paper has been typeset from a \LaTeX file prepared by the author.